1

Stereoselective C—C Bond-Forming Reactions Through C(sp^3)—H Bond Insertion of Metal Carbenoids

Aoife M. Buckley[1], Thomas A. Brouder[1], Alan Ford[1], and Anita R. Maguire[2]

[1]*University College Cork, School of Chemistry, Analytical and Biological Chemistry Research Facility, College Road, T12K8AF Cork, Ireland*
[2]*University College Cork, School of Chemistry and School of Pharmacy, Analytical and Biological Chemistry Research Facility, Synthesis and Solid State Pharmaceutical Centre, College Road, T12K8AF Cork, Ireland*
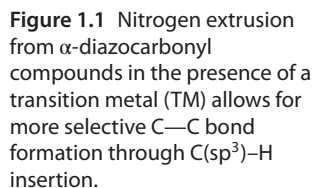
1.1 Introduction

The selective and efficient construction of complex molecules is one of the most challenging goals in organic synthesis. To access such intriguing molecules, innovative methodologies in bond formation are required compared to traditional functional group transformations. It is for this reason that selective functionalization of the ubiquitous but inert C—H bond is of great interest to the chemical community [1–4].

A challenging aspect in organic chemistry for decades has been the stereoselective carbon–carbon bond formation by activation of a C(sp^3)—H bond in the synthesis of pharmaceuticals, natural products, and other industrially relevant targets. A powerful approach to achieve such useful C–H functionalization is via C(sp^3)–H insertion by metal carbenoids [5–8]. Generation of the metal carbenoid can occur through a number of precursors such as diazo compounds, ylide derivatives, hydrazones, and, more recently, triazoles. In this chapter, we will exclusively discuss metal carbenoids derived from α-diazocarbonyl compounds.

In order to take advantage of metal carbenoid-induced C–H insertion, one must consider the reactivity of the electrophilic metal carbenoid. The synthetic utility of the free carbenes is limited by low selectivity in most reactions. In contrast, when nitrogen extrusion is facilitated by a transition metal, the resulting metal carbenoid retains the reaction scope of a free carbene while allowing highly selective transformations to occur (Figure 1.1).

Historically, copper was used as the transition metal source, but few examples of efficient and selective C–H insertion were reported. The key development in C–H insertion was the discovery by the Teyssié group that dirhodium(II) carboxylates catalyzed the intermolecular C–H insertion reaction of ethyl diazoacetate with alkanes [9]. Following this, Wenkert et al. [10] and Taber and Petty [11] highlighted the potential of intramolecular C–H insertion reactions of α-diazocarbonyl compounds to lead to cyclopentanone derivatives. Importantly, it was demonstrated that C–H insertion takes place with retention of

Figure 1.1 Nitrogen extrusion from α-diazocarbonyl compounds in the presence of a transition metal (TM) allows for more selective C—C bond formation through C(sp^3)–H insertion.

configuration at the reacting C—H bond [12]. These early studies triggered four decades of intensive development of selective C–H insertion.

This chapter will explore how the complex relationship between the catalyst and the substrate affects the chemo-, regio-, diastereo-, and enantioselectivity of C—C bond formation through C(sp^3)—H bond insertion by metal carbenoids.

1.2 Diazo Compounds

Diazoalkanes such as diazomethane and diazoethane are challenging to synthesize, inherently unstable, and even explosive in their pure form. Analogs such as phenyldiazomethane exhibit increased stability due to conjugation with the aromatic ring, but still cannot be stored for long periods of time. The presence of a carbonyl group adjacent to the diazo group confers much greater stability, and several diazocarbonyl compounds are stable enough to be stored, and some are commercially available (Figure 1.2).

The reactivity and selectivity of metal carbenoids are affected by the substituents that flank the metal carbene. Diazo carbene precursors are generally classified into three groups according to the nature of their substituents (Figure 1.3).

The terms "acceptor" and "donor" refer to electron-withdrawing and electron-donating character principally through resonance effects. Due to the buildup of positive charge on the carbene carbon during the formation of the carbenoid, ideal substituents will act to stabilize this buildup of positive
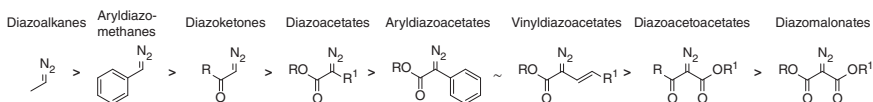

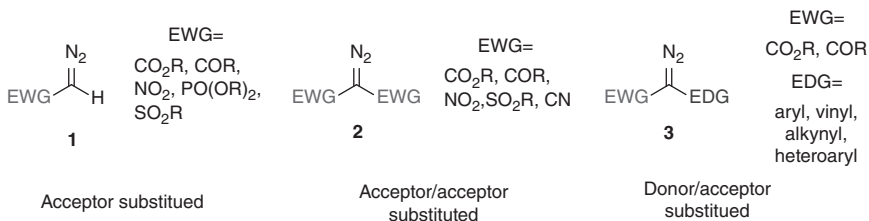**Figure 1.2** Relative reactivity of diazo compounds.

Figure 1.3 Types of diazo compounds.

charge without altering its reactivity. Acceptor groups do little to stabilize the electrophilic carbene center. This leads to limited site selectivity; therefore these compounds are better suited to intramolecular $C(sp^3)$–H insertion than intermolecular $C(sp^3)$–H insertion. Conversely, the presence of an electron-donating group confers a degree of stability to the metal carbenoid. Aryldiazoacetate derivatives are the most commonly used donor/acceptor-substituted α-diazocarbonyl precursors for intermolecular C–H insertion.

1.3 Mechanistic Understanding

The mechanism of transition metal C–H insertion has been thoroughly investigated by several research teams [13–17], and a simplified catalytic cycle is shown in Figure 1.4. The metal ligated catalyst (ML_n) coordinates with the diazo compound leading to nitrogen extrusion and formation of a metal carbenoid. This metal carbenoid then undergoes C–H insertion to form the new carbon–carbon bond.

For C–H insertion reactions to be synthetically useful, high chemo-, regio-, diastereo-, and enantioselectivity are necessary. To be able to achieve such control, a more detailed understanding of the mechanism is required. Several hypotheses on the mechanism have been proposed for the rhodium-catalyzed C–H insertion [13, 18–20]. Doyle suggested a three-centered concerted mechanism, which was advanced by Nakamura's theoretical studies [15]; however intermolecular density functional theory (DFT) computational studies carried out by Davies have disputed this hypothesis in certain cases [17].

Initially, the metal carbenoid intermediate (Figure 1.5) is generated through (i) the σ-bonding from the carbene carbon to the metal atom and (ii) the π-backdonation from the filled metal d-orbitals to the carbene carbon that possesses a vacant p-orbital. This vacant 2p orbital leads to the formation of a highly electrophilic metal carbenoid [21].

The ligands coordinated to the metal can alter the electrophilicity of the metal carbenoid. A more reactive carbenoid is observed when electron-withdrawing ligands are present on the metal due to reduced backbonding to the vacant
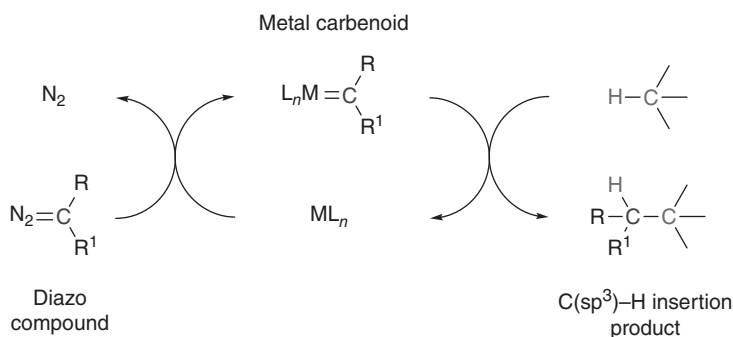

Figure 1.4 Simplified catalytic cycle of $C(sp^3)$–H insertion via metal carbenoid formation.
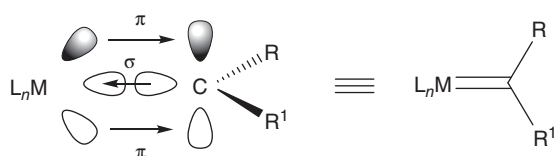
Figure 1.5 Bonding in a metal carbenoid.

carbene p-orbital. Alternatively, a less reactive carbenoid is generated with the use of electron-donating groups. There is a balance that needs to be struck between reactivity and selectivity of the carbenoid.

Once the carbenoid is formed, it undergoes C–H insertion through the overlap of the empty p-orbital of the metal carbenoid with the σ-orbital of the C—H bond. This involves two steps: (i) hydride transfer and (ii) carbon–carbon bond formation. It is believed that these steps can occur in an asynchronous concerted three-centered transition state (**TS-I**; Scheme 1.1) or with considerable hydride transfer character, which is likely to be followed by rapid carbon–carbon bond formation (Scheme 1.2) [17].
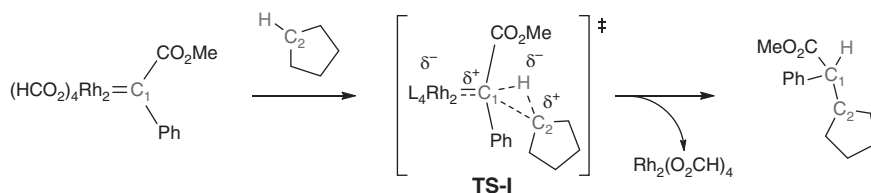
Scheme 1.1 Less activated C(sp³)—H bonds proceed via an asynchronous concerted three-centered transition state.
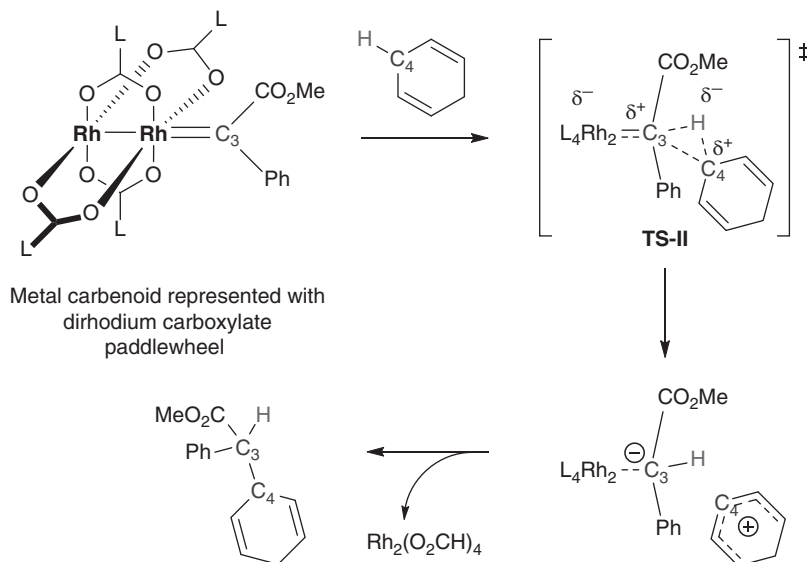
Scheme 1.2 More activated C(sp³)—H bonds proceed with a hydride transfer characteristic and a more asynchronous mechanism.

Computational studies by Davies and coworkers suggest that reactions of donor/acceptor carbenoids with less activated C—H bonds (e.g. cyclopentane) more closely resemble to the concerted asynchronous mechanism, while more activated C—H bonds (e.g. cyclopentadiene) show an appreciable degree of hydride transfer in a somewhat earlier transition state (**TS-II**; Scheme 1.2). For a donor/acceptor-substituted α-diazocarbonyl compound, C–H insertion is believed to be the rate-limiting step as a higher activation energy is calculated for C–H insertion over nitrogen extrusion [15]; however, DFT calculations have shown for acceptor-substituted diazo compounds that the nitrogen extrusion is the rate-limiting step for secondary C–H insertion [17]. Although these computational studies have modeled intermolecular experiments, the same hypothesis has been applied to the understanding of intramolecular C–H insertion reactions.

While rhodium(II) catalysts have been the most widely researched transition metal complexes for C–H insertion, in recent years, attention has also turned to the prospect of efficient and selective catalysts from other metals including copper, iridium, ruthenium, iron, and gold, for which a similar C–H insertion mechanistic pathway is anticipated [22].

1.4 Catalysts

Efficient and selective C–H insertion requires a carbenoid intermediate of appropriate reactivity and electrophilicity. Judicious choice of metal–ligand combination is essential to strike the right balance between reactivity and selectivity. While carbenoids can be generated with a number of transition metals, some like the coinage metals (gold, silver) are too reactive, thus rendering selectivity difficult to achieve [23]. Others such as ruthenium are too stable to undergo C–H insertion. Typically, copper and rhodium are the transition metals of choice for C–H insertion reactions.

1.4.1 Copper

Before the advent of dirhodium tetraacetate, virtually all of the early literature relating to metal-catalyzed carbenoid reactions reports the use of copper complexes [24–26]. Synthetic utility of these copper-based catalysts was limited to geometrically rigid systems, and yields were moderate at best [24]. Since the first reported copper-catalyzed enantioselective C–H insertion reactions by Sulikowski and coworker [27], this area of metal catalysis has seen renewed interest.

1.4.1.1 Bisoxazoline and Schiff Base

The most widely studied copper-based ligands are the C_2-symmetric bisoxazolines. The success of such ligands can be attributed to the symmetry about the C_2 axis, which reduces the number of possible transition states for a given reaction. In addition, they also possess a conformationally constrained metal chelate
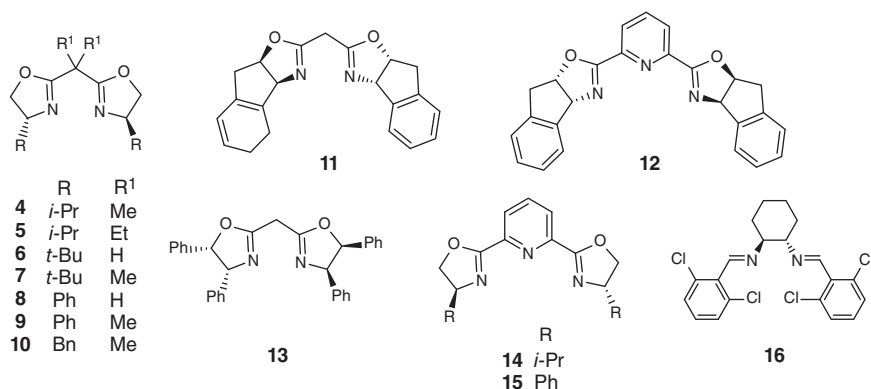
R | R^1
4 | *i*-Pr | Me
5 | *i*-Pr | Et
6 | *t*-Bu | H
7 | *t*-Bu | Me
8 | Ph | H
9 | Ph | Me
10 | Bn | Me

Figure 1.6 A selection of commercially available bisoxazoline ligands (**4–15**) and a Schiff base ligand (**16**).

structure where the stereocenter that affects enantiocontrol resides on the carbon adjacent to the metal-coordinating nitrogen of the oxazoline ring, thereby directly influencing the stereochemical outcome of the reaction.

Much of the extensive range of bisoxazoline ligands synthesized to date has been covered by Desimoni et al. [28]; a selection of the most commonly used and commercially available ligands is presented in Figure 1.6.

The ligands are usually reacted *in situ* with a copper source such as copper chloride or copper triflate. Bisoxazoline complexes have been employed in both intra- and intermolecular C–H insertion with enantioinduction of up to 98% ee being achieved in the synthesis of cyclopentanones **18** and thiopyrans **19** (Scheme 1.3) [29, 30].
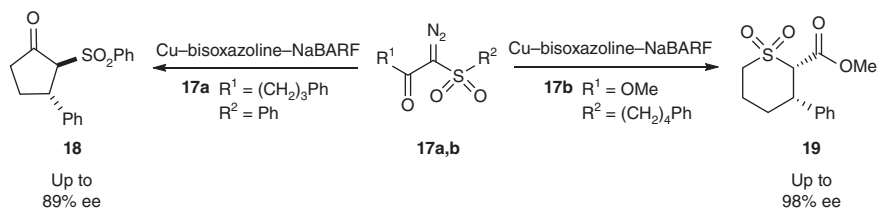
Scheme 1.3 Cyclopentanone and thiopyran formation using a copper-bisoxazoline catalytic system.

A further example of copper-catalyzed asymmetric C–H insertion involves the C_2-symmetric Schiff base copper complex **16,** which has shown moderate success in the enantioselective synthesis of D-*threo*-methylphenidate [31].

1.4.2 Rhodium

Since the introduction of dirhodium tetraacetate in the early 1980s [9], rhodium has been the transition metal of choice for a wide range of carbene-mediated transformations and specifically for asymmetric C–H insertion due to its superior selectivity and efficiency compared with other metals. Key to the success

of dirhodium complexes is their highly symmetrical paddlewheel conformation [32]. Within this framework, the dirhodium-bridged cage forms a "lantern" structure. Only one of the two rhodium atoms serves as a binding site for the diazo-generated carbene. The second rhodium atom acts as an electron sink, thereby increasing electrophilicity of the carbene and facilitating cleavage of the rhodium carbene bond upon reaction completion.

1.4.2.1 Rhodium(II) Carboxylates

Following the success of rhodium tetraacetate, a wide range of rhodium(II) carboxylates were investigated. Rhodium carboxylates are particularly effective in carbene transfer reactions due to their electron-deficient character. Since the first use of a chiral rhodium(II) catalyst, $Rh_2(S\text{-BSP})_4$ (**20**), by McKervey and coworkers [33], the design and synthesis of novel rhodium(II) carboxylate catalysts has been the subject of intensive research. Only a limited number of chiral templates have produced consistently high enantioselectivities, and a selection of these will be discussed here.

Davies has reported excellent results with chiral dirhodium tetraprolinates and donor/acceptor-substituted carbenoids at −78 °C [34]. The tetraprolinates were shown to have enhanced enantioselectivity in nonpolar solvents, thought to be the result of solvent-induced orientation of the prolinate ligands, leading to a complex with overall D_2 symmetry [34, 35]. This led to the development of hydrocarbon-soluble $Rh_2(S\text{-TBSP})_4$ (**21**) and $Rh_2(S\text{-DOSP})_4$ (**22**) catalysts (Figure 1.7).

$Rh_2(S\text{-DOSP})_4$ in particular has been a valuable asset in achieving high enantioinduction in the challenging field of intermolecular C−H insertion [36]. A second generation of more finely tuned catalysts included $Rh_2(S\text{-biTISP})_4$ (**24**) and $Rh_2(S\text{-biDOSP})_4$ (**25**), which possess a rigid bridge structure locked in a D_2-symmetric conformation [37]. A further class of catalysts was developed with cyclopropanecarboxylate ligands (**26–28**), which have shown excellent selectivity and asymmetric induction in intermolecular C−H insertion [38, 39].

Hashimoto and Ikegami developed rhodium(II) carboxylate catalysts built around N-phthaloyl-(S)-amino acid templates, the most successful of which has been $Rh_2(S\text{-PTTL})_4$ (**31**), and later a second generation of catalysts that extended the phthalimide moiety by an additional benzene ring [40, 41]. Davies
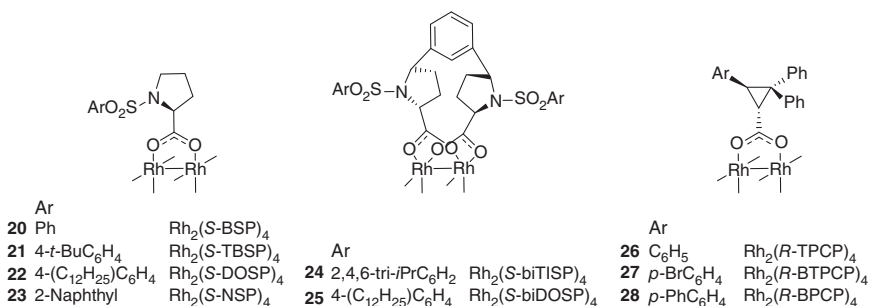

20 Ph	$Rh_2(S\text{-BSP})_4$				
21 4-t-BuC$_6$H$_4$	$Rh_2(S\text{-TBSP})_4$	**Ar**		**Ar**	
22 4-(C$_{12}$H$_{25}$)C$_6$H$_4$	$Rh_2(S\text{-DOSP})_4$	**24** 2,4,6-tri-iPrC$_6$H$_2$	$Rh_2(S\text{-biTISP})_4$	**26** C$_6$H$_5$	$Rh_2(R\text{-TPCP})_4$
23 2-Naphthyl	$Rh_2(S\text{-NSP})_4$	**25** 4-(C$_{12}$H$_{25}$)C$_6$H$_4$	$Rh_2(S\text{-biDOSP})_4$	**27** p-BrC$_6$H$_4$	$Rh_2(R\text{-BTPCP})_4$
				28 p-PhC$_6$H$_4$	$Rh_2(R\text{-BPCP})_4$

Figure 1.7 Commonly used prolinate- and cyclopropane-derived rhodium(II) carboxylate catalysts.

R
29 Me $Rh_2(S\text{-PTA})_4$
30 *i*-Pr $Rh_2(S\text{-PTV})_4$
31 *t*-Bu $Rh_2(S\text{-PTTL})_4$
32 Bn $Rh_2(S\text{-PTPA})_4$
33 Ph $Rh_2(S\text{-PTPG})_4$
34 CEt$_3$ $Rh_2(S\text{-PTTEA})_4$
35 Adamantyl $Rh_2(S\text{-PTAD})_4$

R
36 Me $Rh_2(S\text{-BPTA})_4$
37 *t*-Bu $Rh_2(S\text{-BPTTL})_4$

R   X
38 *t*-Bu   F $Rh_2(S\text{-TFPTTL})_4$
39 *t*-Bu   Cl $Rh_2(S\text{-TCPTTL})_4$
40 Adamantyl Cl $Rh_2(S\text{-TCPTAD})_4$
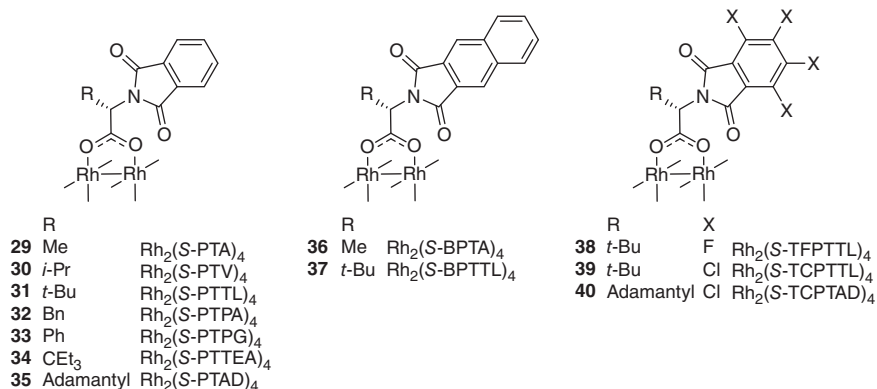
Figure 1.8 Commonly used phthaloyl-derived rhodium(II) carboxylate catalysts.

has reported high levels of asymmetric induction using the phthaloyl catalyst with the adamantylglycine-derived $Rh_2(S\text{-PTAD})_4$ (**35**) [42]. Recently a third generation of phthaloyl catalysts has been introduced, $Rh_2(S\text{-TFPTTL})_4$ (**38**) and $Rh_2(S\text{-TCPTTL})_4$ (**39**), incorporating halogens on the phthalimide ring. These have shown excellent enantioselectivity and reactivity, high turnovers, and low catalyst loadings [43–46] (Figure 1.8).

1.4.2.2 Rhodium(II) Carboxamidates

First described by Dennis et al. [47], chiral rhodium(II) carboxamidates are constructed from lactams derived from amino acids and possess four carboxamidate ligands around the dirhodium core with two oxygen and two nitrogen donor atoms. Four different isomers are possible due to the unsymmetrical bonding of the carboxamidate ligands to the rhodium core. The most dominant isomer formed after ligand exchange with rhodium acetate is the 2,2-cis configuration (85%) [48].

In general, rhodium(II) carboxamidates are less reactive toward α-diazo-carbonyl compounds than rhodium(II) carboxylates; thus higher selectivity is possible. This is especially true for acceptor-substituted carbenoids derived from α-diazoesters and α-diazoacetamides.

A wide range of carboxamide catalysts have been described by Doyle and coworkers, including the complexes **41**–**48** shown in Figure 1.9. These catalysts have proven very effective in cyclizations of specific substrate types.
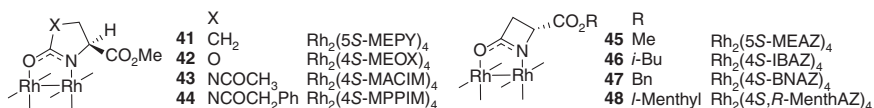

X
41 CH$_2$ $Rh_2(5S\text{-MEPY})_4$
42 O $Rh_2(4S\text{-MEOX})_4$
43 NCOCH$_3$ $Rh_2(4S\text{-MACIM})_4$
44 NCOCH$_2$Ph $Rh_2(4S\text{-MPPIM})_4$

R
45 Me $Rh_2(5S\text{-MEAZ})_4$
46 *i*-Bu $Rh_2(4S\text{-IBAZ})_4$
47 Bn $Rh_2(4S\text{-BNAZ})_4$
48 *l*-Menthyl $Rh_2(4S,R\text{-MenthAZ})_4$

Figure 1.9 Commonly used rhodium(II) carboxamidate catalysts.

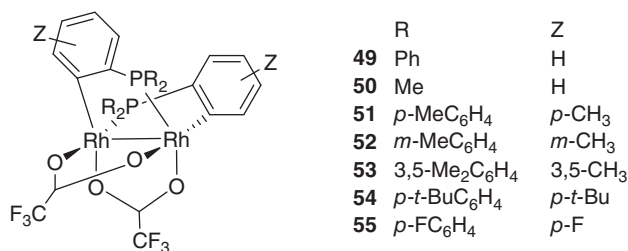|	R	Z
49	Ph	H
50	Me	H
51	*p*-MeC$_6$H$_4$	*p*-CH$_3$
52	*m*-MeC$_6$H$_4$	*m*-CH$_3$
53	3,5-Me$_2$C$_6$H$_4$	3,5-CH$_3$
54	*p*-*t*-BuC$_6$H$_4$	*p*-*t*-Bu
55	*p*-FC$_6$H$_4$	*p*-F

Figure 1.10 Ortho-metalated rhodium(II) catalysts utilized in C–H insertion.

1.4.2.3 Ortho-metalated Complexes

Unusually these dirhodium catalysts, which were first reported by Cotton et al. [49], do not derive chirality from stereogenic ligands but instead possess backbone chirality. They are made up of two ortho-metalated arylphosphines and two carboxylate ligands arranged in a cis confirmation (Figure 1.10). They have had reasonable success in the cyclizations of α-diazoketones via C–H insertion (up to 74% ee) [50].

1.4.3 Iridium and Ruthenium

In 2009, Suematsu and Katsuki described the first example of iridium-catalyzed asymmetric C–H insertion with excellent enantioselectivities of up to 97% ee using complex **57** [51]. Iridium bisoxazoline **58** [52] and iridium porphyrin complex **59** [53, 54] have also found use in intermolecular C–H insertion allowing excellent yields and enantioselectivities (up to 99% ee) to be achieved (Figure 1.11).

Ruthenium complexes **61–64** have been used to catalyze intramolecular C–H insertion of alkyl diazomethanes with excellent diastereoselectivity. Few examples of ruthenium-catalyzed enantioselective C–H insertion reactions are reported, but Che and coworkers have published an intermolecular C(sp³)–H insertion catalyzed by **60**, delivering a chiral product with 92% ee [55]. This group has also shown that diastereoselective synthesis of β-lactams can be carried out via [RuCl$_2$(*p*-cymene)]$_2$-catalyzed cyclization of α-diazoacetamides in good to excellent yields and asymmetric induction of up to 55% ee has been achieved with the use of pyridine bisoxazoline **15** together with this catalyst [56].

1.5 Intramolecular C(sp³)—H Bond Insertion

Intramolecular C–H insertion was not regarded as an efficient transformation until Wenkert et al. [10] and Taber and Petty [11] almost simultaneously, but
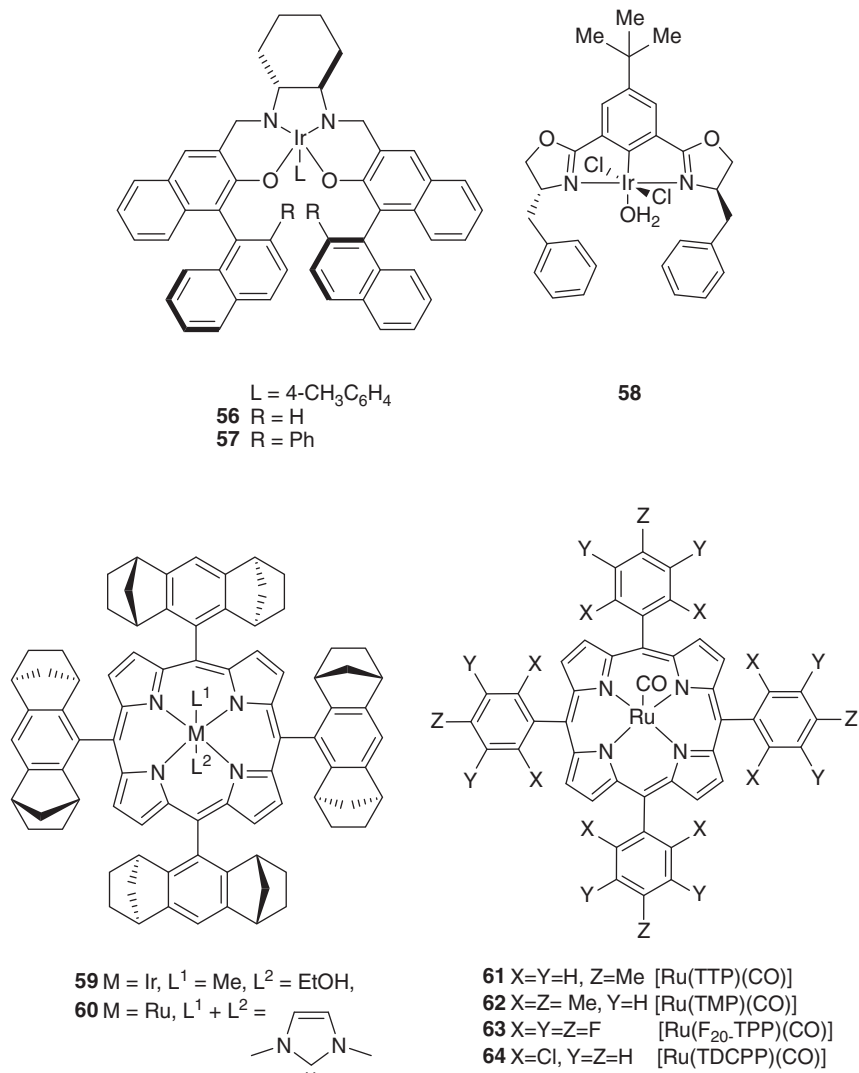
L = 4-CH$_3$C$_6$H$_4$
56 R = H
57 R = Ph

58

59 M = Ir, L^1 = Me, L^2 = EtOH,
60 M = Ru, L^1 + L^2 =

61 X=Y=H, Z=Me [Ru(TTP)(CO)]
62 X=Z= Me, Y=H [Ru(TMP)(CO)]
63 X=Y=Z=F   [Ru(F$_{20}$.TPP)(CO)]
64 X=Cl, Y=Z=H [Ru(TDCPP)(CO)]

Figure 1.11 Iridium and ruthenium catalysts utilized in C–H insertion.

independently, reported the rhodium-catalyzed cyclization of α-diazoketones, **65** and **67**, respectively, in the early 1980s. This work, which was preceded by the use of dirhodium tetracarboxylates in intermolecular C–H insertion by Teyssié, allowed intramolecular C–H insertion to emerge as a powerful synthetic pathway for the construction of five-membered rings. Taber recognized the potential for asymmetric induction in this transformation by introducing chiral auxiliaries to the α-diazoketone precursors [57], followed by McKervey and coworkers who reported the first use of chiral dirhodium catalysts in asymmetric intramolecular C–H insertion to provide cyclopentanone **70** with a modest 12% ee (Scheme 1.4) [33].
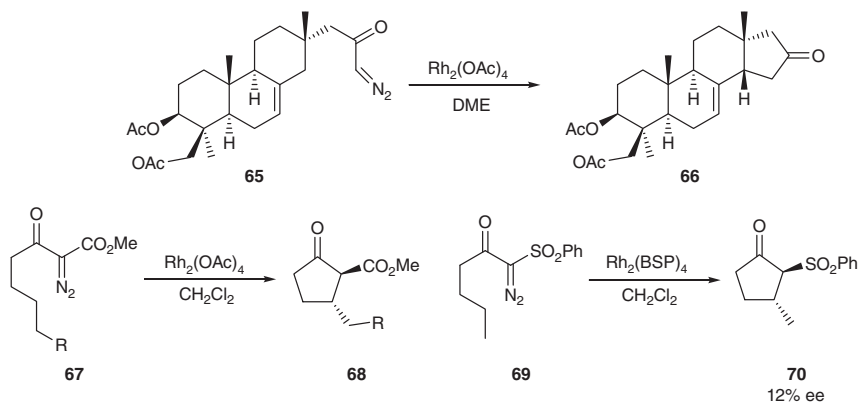
Scheme 1.4 Seminal work in intramolecular C–H insertion by Wenkert, Taber, and McKervey.

Since these seminal reports, the field of metal-catalyzed asymmetric intramolecular insertion into C—H bonds has seen major advances and become a reliable methodology for C—C bond formation. For clarity, this chapter will be organized in terms of chemo-, regio-, stereo-, and enantioselectivity with rhodium-catalyzed C–H insertion dominating the literature in this field.

1.5.1 Chemoselectivity

1.5.1.1 Catalyst Effects

The preference of carbenoids to undergo C–H insertion over other carbene-based transformations is of great interest to synthetic chemists. In rhodium-catalyzed carbene-mediated transformations, selectivity for C–H insertion has been found to be dependent on the catalyst, specifically the electronic properties of the ligands. This was demonstrated by Padwa, Doyle, and coworkers in a series of intramolecular competition experiments [58, 59]. The α-diazoketone **71** has the potential to undergo cyclopropanation or C(sp³)–H insertion; it was found that C–H insertion was the only reaction pathway observed when using the highly electrophilic carbenoid derived from $Rh_2(pfb)_4$ (**74**). In contrast, the more electron-rich carbenoid derived from $Rh_2(cap)_4$ (**75**) led to a switch in chemoselectivity, favoring cyclopropanation completely. The electronic properties of $Rh_2(OAc)_4$ (**76**) fall somewhere between the other two catalysts, so very little chemoselectivity was observed (Figure 1.12 and Scheme 1.5).
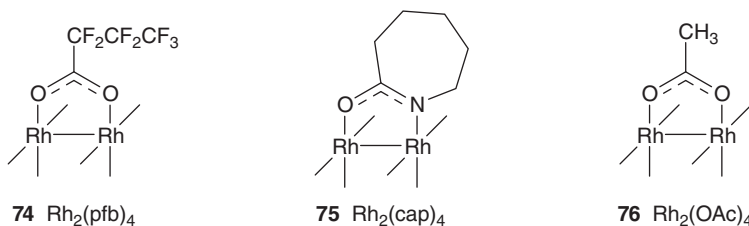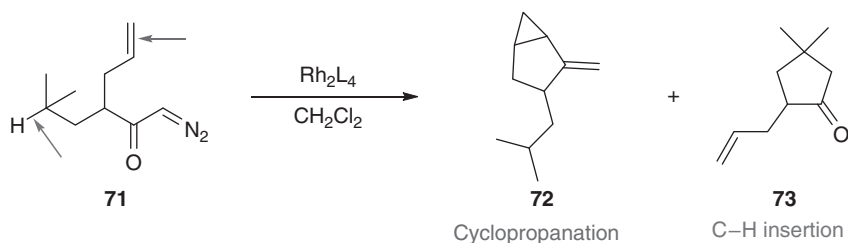

74 $Rh_2(pfb)_4$ **75** $Rh_2(cap)_4$ **76** $Rh_2(OAc)_4$

Figure 1.12 Achiral rhodium catalysts.

Entry	Catalyst	Ratio 72 : 73
1	Rh$_2$(pfb)$_4$	0 : 100
2	Rh$_2$(OAc)$_4$	44 : 56
3	Rh$_2$(cap)$_4$	100 : 0

Scheme 1.5 Ligand-dependent chemoselectivity between cyclopropanation and C–H insertion.

Another example of ligand-dependent chemoselectivity was observed when α-diazoacetamide **77**, which possesses sites for C–H insertion and aromatic addition, was subjected to rhodium catalysis. In this experiment, C–H insertion was the preferred reaction pathway when using Rh$_2$(cap)$_4$, while Rh$_2$(pfb)$_4$ produces mainly the aromatic addition product. No insertion into the *tert*-butyl group was observed (Scheme 1.6). Although only two examples are shown here, an extensive series of these competition experiments were conducted, which highlighted reactivity trends based on catalyst selection (Figures 1.13 and 1.14) [60].
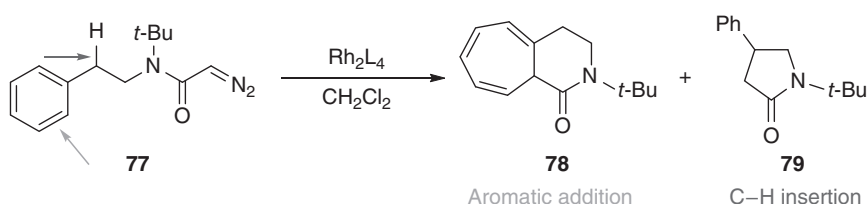
Entry	Catalyst	Ratio 78 : 79
1	Rh$_2$(pfb)$_4$	95 : 5
2	Rh$_2$(OAc)$_4$	68 : 32
3	Rh$_2$(cap)$_4$	3 : 97

Scheme 1.6 Ligand-dependent chemoselectivity between aromatic addition and C–H insertion.

1.5.1.2 Substrate Effects

Another factor that impacts selectivity for C–H insertion over other reaction pathways is the substitution pattern of the α-diazocarbonyl substrate. Typically acceptor-substituted compounds (bearing only one electron withdrawing group
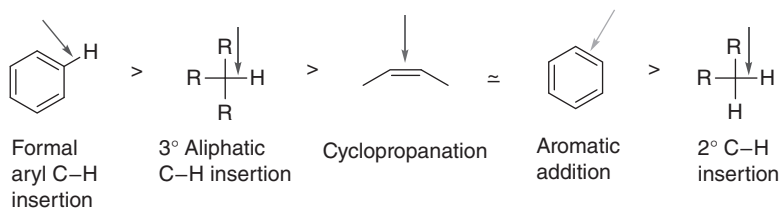
Figure 1.13 Reactivity trends for highly electrophilic carbenoids such as those derived from $Rh_2(pfb)_4$.
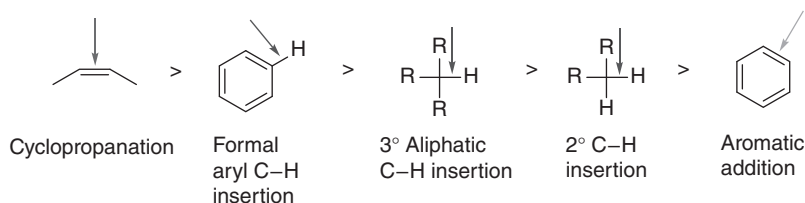

Figure 1.14 Reactivity trends for more electron-rich carbenoids such as those derived from $Rh_2(cap)_4$.

[EWG] α to the diazo moiety) lead to more reactive carbenoid intermediates. This may allow homocoupling to compete as a side reaction. This homocoupling side reaction is strongly disfavored for less reactive acceptor/acceptor or donor/acceptor α-diazocarbonyl compounds (Scheme 1.7).
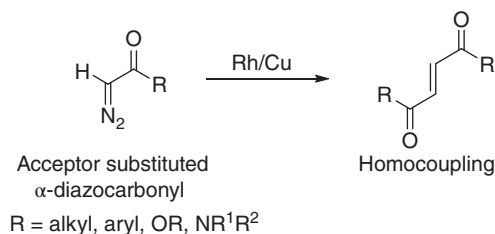

Scheme 1.7 Homocoupling may occur between acceptor-substituted α-diazocarbonyl compounds.

Interestingly, Padwa and Moody showed that if a hydroxyl group is present within the substrate, O–H insertion will dominate over any other carbenoid-mediated transformation, regardless of the dirhodium catalyst employed (Scheme 1.8). While yields varied, O–H insertion was the sole product obtained with no evidence for cyclopropanation, aromatic addition, or aliphatic or aromatic C–H insertion [61].

Wee and coworkers designed a study made up of 11 α-diazoanilides **82** with varying *N*-substituents to investigate alkyl vs. aryl C–H insertion (Scheme 1.9). In all cases, alkyl C–H insertion was the only pathway observed (e.g. **83**). In contrast, when the α-diazoester moiety was changed to a phenylsulfone or a methyl ketone, formal aromatic C–H insertion was observed exclusively (one
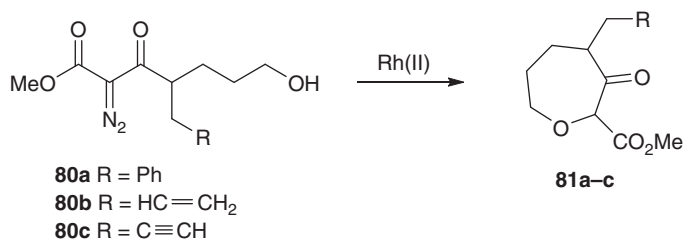
Scheme 1.8 O–H insertion is the dominant carbenoid-mediated reaction pathway when a hydroxy group is present in a molecule.
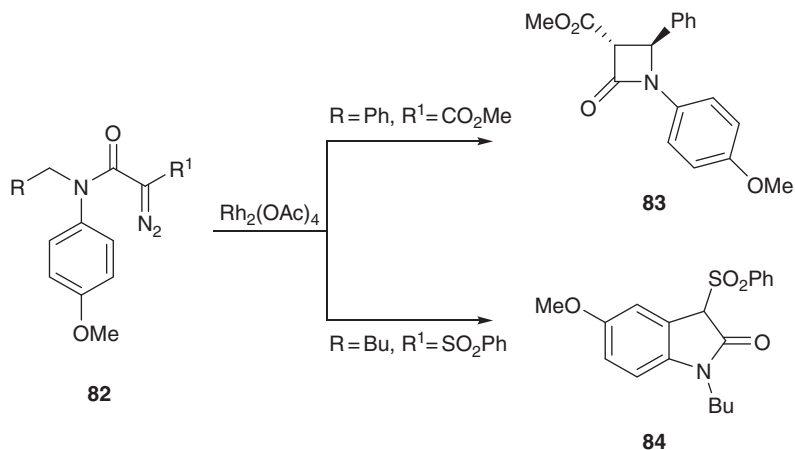

Scheme 1.9 Alkyl vs. aryl C–H insertion depending on the electronic properties of the group α to the diazo moiety.

example, **84**). This can be rationalized as the more electron-withdrawing acetyl or phenylsulfonyl group leads to a more electrophilic carbenoid when compared with an ester-derived carbenoid [62]. It should be noted that while this reaction pathway is frequently referred to as "aromatic C–H insertion," strictly speaking it should not be, as the mechanism is aromatic substitution rather than C–H insertion.

It has also been shown that the electronic properties of the aryl ring play a role in the chemoselectivity of a carbenoid reaction, with the strongly electron-withdrawing nitro substituent disfavoring aromatic addition and promoting C–H insertion as the dominant reaction pathway (Scheme 1.10) [59].

1.5.2 Regioselectivity

Following Taber's investigations [11, 12, 63], it was well established that intramolecular C–H insertion occurs to preferentially form five-membered ring compounds. This fact has been exploited to construct cyclopentanones, dihydrofurans, γ-lactones, and γ-lactams among other five-membered carbo- and heterocyclic ring systems.
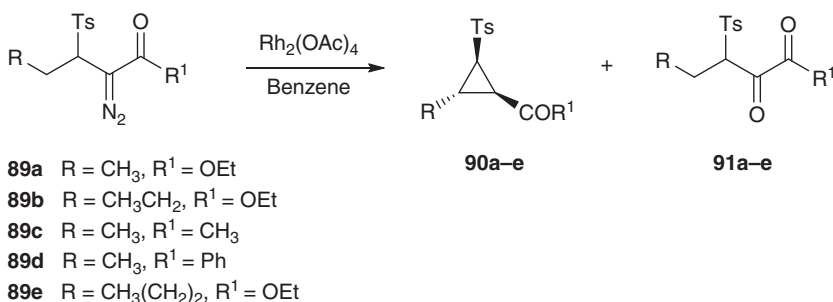
Scheme 1.10 Electronic properties of the aryl ring play a role in chemoselectivity.
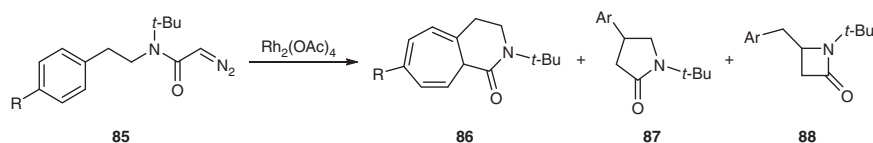
Entry	85	R	Ratio 86 : 87 : 88
1	a	OMe	76 : 24 : 0
2	b	NO$_2$	8 : 77 : 15

Although 1,5 C–H insertion is the favored reaction pathway due to entropic factors, steric or electronic factors can override this preference to form larger or smaller ring sizes. In general, 1,4 C–H insertion can occur if the C—H bond is activated by a neighboring heteroatom, usually nitrogen or oxygen, while 1,6 C–H insertion has been observed for more structurally rigid systems. Even 1,3 C–H insertion has been reported for β-tosyl α-diazocarbonyl compounds.

1.5.2.1 Formation of Three-Membered Rings

While three-membered rings can be constructed through C–H insertion in geometrically rigid structures, only one example of three-membered ring formation in a freely rotating system has been reported to date. Wang and coworkers found that α-diazocarbonyl compounds with a β-tosyl functionality undergo C–H insertion to give a cyclopropane ring with excellent diastereoselectivity (Scheme 1.11) [64]. When the reaction is performed under strict oxygen-free conditions to prevent formation of oxidation product **91**, 1,3 C–H insertion is the major reaction pathway observed in all but one case. Interestingly, α-diazocarbonyl compound **89e** has the potential to undergo 1,3 C–H insertion or 1,5 C–H insertion. Using Rh$_2$(OAc)$_4$ as the catalyst, an equal distribution of insertion products is observed, but if a catalyst with more electron-withdrawing ligands such as Rh$_2$(tfa)$_4$ is employed, 1,3 C–H insertion is favored. This study demonstrates the dramatic effect of neighboring groups and catalyst selection on regioselectivity. At the time of writing, 1,3 C–H insertion has only been reported with achiral catalysts.


89a R = CH$_3$, R^1 = OEt
89b R = CH$_3$CH$_2$, R^1 = OEt
89c R = CH$_3$, R^1 = CH$_3$
89d R = CH$_3$, R^1 = Ph
89e R = CH$_3$(CH$_2$)$_2$, R^1 = OEt

Scheme 1.11 1,3 C–H insertion is possible in freely rotating α-diazocarbonyl compounds with a β-tosyl functionality.

1.5.2.2 Formation of Four-Membered Rings

The most common four-membered rings formed through C–H insertion are β-lactones and β-lactams. The selective synthesis of these structural motifs is of great interest as they are found in many and biologically active compounds. The main barrier to the formation of four-membered rings from C–H insertion reactions is the preference for 1,5 C–H insertion when both sites of insertion are available. It is thus necessary to restrict access to the δ-C–H insertion site either electronically or sterically in order to force 1,4-insertion.

Attempts to synthesize β-lactones have been challenging, as γ-lactones are almost always the exclusive reaction products in C–H insertion reactions of α-diazoacetates. A notable exception to this trend was reported by Doyle when he showed the cyclization of alkyl phenyldiazoacetates, which produce β-lactones as the major reaction product (Scheme 1.12). In the examples shown here, Rh$_2$(S-DOSP)$_4$ is employed to produce β-lactones **93** and **95** in good yields and modest enantioselectivity with only trace amounts of the γ-lactone product detected [65].
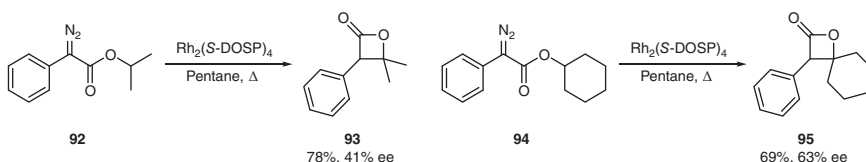

Scheme 1.12 β-Lactone synthesis from alkyl phenyldiazoacetates.

This regioselectivity can be suppressed when a highly activated γ C—H bond is available for insertion. In Scheme 1.13, no β-lactone is formed; instead the γ-lactone **98** is formed in 94% yield and excellent enantioselectivity.
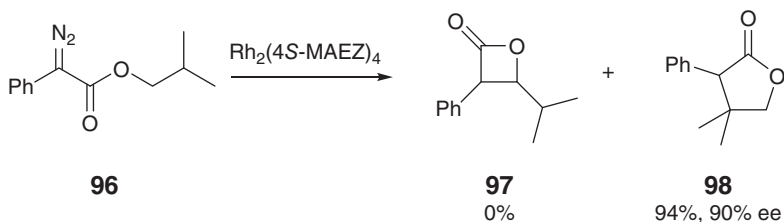
Scheme 1.13 β-Lactone synthesis is suppressed when a highly activated γ C—H bond is available.

This work has been expanded further by Davies and coworkers [46] and Bach and coworker [66] to show that it is not only the substitution at the ester site that influences the regioselectivity but also the substitution on the α-aryl ring. Both groups observed that an ortho substituent on the aryldiazoacetate promoted 1,4-insertion, while Davies reported that the ortho substituent is essential to achieve any β-lactone product when performing methyl C–H insertion and enantioselectivity is enhanced in the presence of a methoxy group on the aryl ring (Scheme 1.14).

Scheme 1.14 Ortho-substitution on the aryl ring is essential for β-lactone synthesis when inserting into a methyl C—H bond.
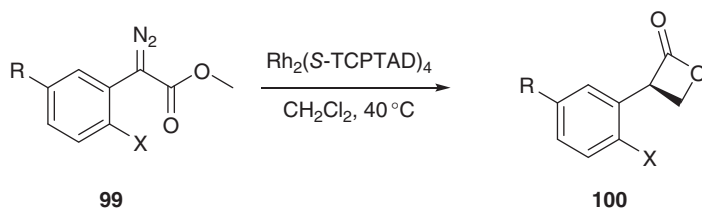
Entry	99	R	X	%Yield 100	%ee 100
1	a	H	H	—	—
2	b	H	Br	53	61
3	c	OMe	I	67	92

The β-lactam ring is arguably one of the most pharmaceutically important heterocycles in modern medicine due to its presence in the essential broad-spectrum antibiotics such as penicillins and cephalosporins. Intramolecular C–H insertion of α-diazoacetamides can be exploited to generate β-lactams as the amide nitrogen activates the adjacent C—H bond toward insertion by a carbenoid.

The first report of β-lactam formation through C–H insertion came from Corey and Felix [67], but the first enantioselective β-lactam synthesis by C–H insertion was published by Doyle et al. [68]. In this report, the efficiency of β-lactam formation was dependent on the substituents on the *N*-alkyl chain of the α-diazoacetamide precursor, never reaching over 25% yield with any chiral catalyst and moderate enantioselectivity of up to 80% ee in the case of **103a** using $Rh_2(4S\text{-MEOX})_4$ (Scheme 1.15).
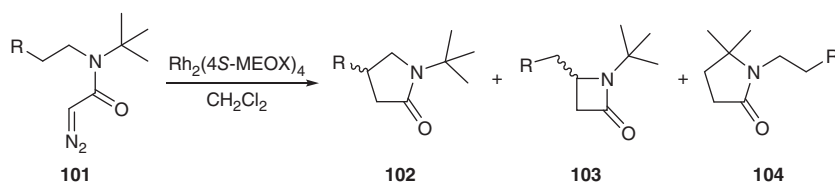
Entry	101	R	%Yield 102	%ee 101	%Yield 103	%ee 103	%Yield 104	%ee 104
1	a	Et	91	71	9	80	0	—
2	b	*i*-Pr	82	69	18	65	0	—
3	c	OEt	100	78	0	—	0	—

Scheme 1.15 First report of enantioselective β-lactam synthesis.

Due to the preference of freely rotating alkyldiazoacetamides to undergo 1,5 C–H insertion, Doyle investigated enantioselective synthesis of β-lactams using more conformationally constrained α-diazoacetylazacycloalkanes. While no success was reported with pyrrolidine-, piperidine-, or morpholine-derived α-diazoacetamides, the azacycloheptane and azacyclooctane analogs displayed excellent regioselectivity with >99 : 1, β:γ lactam formation, excellent yields,
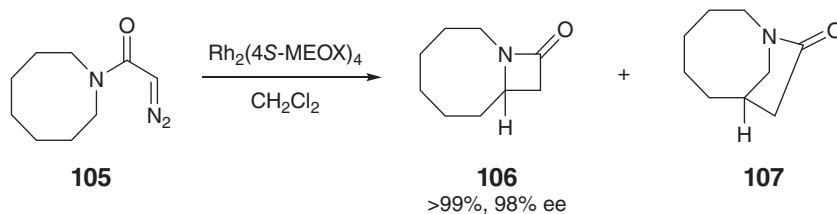
Scheme 1.16 β-Lactam synthesis from an azacyclooctane-derived α-diazoacetamide.

and very high enantioselectivities (Scheme 1.16) [69]. More examples of chiral β-lactam generation through C–H insertion exist, but all show a high dependence on the substitution pattern of the α-diazoacetamide as well as catalyst sensitivity [70].

1.5.2.3 Formation of Five-Membered Rings

The early studies by Taber and coworkers [11, 57, 63] and Doyle et al. [71] have demonstrated that a carbene will insert into a tertiary C—H bond over a secondary C—H bond and primary C–H insertion is the least favorable. This is because a buildup of positive charge occurs on the carbon at the insertion site; therefore a substitution pattern that can better stabilize the positive charge will promote the insertion process (Scheme 1.17). This selectivity can also be influenced by the electronic properties of the catalyst [19].
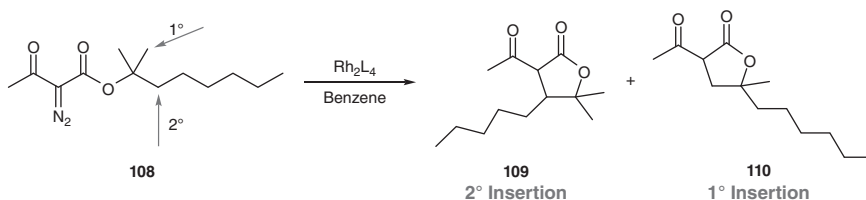

Entry	Catalyst	Ratio 109 : 110
1	Rh$_2$(pfb)$_4$	34 : 66
2	Rh$_2$(OAc)$_4$	75 : 25
3	Rh$_2$(cap)$_4$	92 : 8

Scheme 1.17 The preference for insertion to occur into 1° vs. 2° bonds can be influenced by the ligands on a catalyst.

1.5.2.4 Formation of Six-Membered Rings

The formation of six-membered rings through C–H insertion has been shown to be strongly dependent on the nature of the α-diazocarbonyl precursor. It was found that by activating the C–H insertion site with an adjacent heteroatom, six-membered rings could be constructed. Expanding on earlier work by McKervey and Ye [72], Hashimoto and coworkers have reported the chemo-, stereo-, and enantioselective synthesis of six-membered oxygen-containing heterocycles through 1,6 C–H insertion [73]. The tetrahydropyran **112** was synthesized
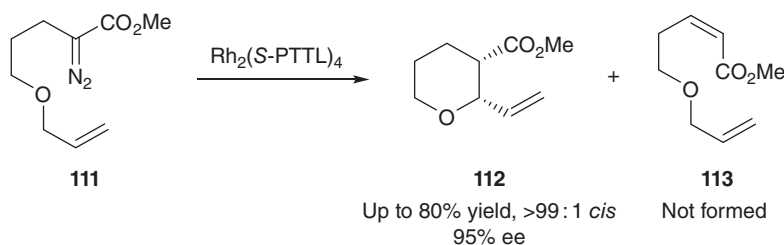
Scheme 1.18 Diastereo- and enantioselective synthesis of a tetrahydropyran through 1,6 C–H insertion.

in up to 95% ee and complete cis diastereoselectivity using $Rh_2(S\text{-PTTL})_4$ (Scheme 1.18). When the reaction was carried out in diethyl ether at −60 °C, there was no evidence for the competing β-hydride elimination product **113**.

α-Heteroatom activation is not always necessary to induce 1,6 C–H insertion as has been demonstrated by Novikov and coworkers [74, 75], Taber et al. [76], and Du Bois and coworkers [77] in the synthesis of six-membered cyclic sulfones, sultones, and cyclohexanones.

Novikov and Taber have studied the effects on regioselectivity of varying substitution patterns on the α-diazocarbonyl substrate. Novikov and coworkers looked at changing the substitution on the carbon adjacent to the sulfone moiety and at the insertion site. Substitution α to the sulfone favored 1,5 C–H insertion, while a longer chain length promoted thiopyran formation through 1,6 C–H insertion (Scheme 1.19) [75].
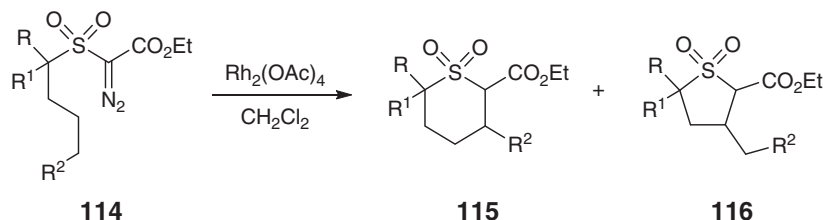
| Entry	114	Substituents	%Yield 115	%Yield 116
1	a	$R = H, R^1 = H, R^2 = Me$	65	9
2	b	$R = H, R^1 = H, R^2 = H$	2	25
3	c	$R = Me, R^1 = Me, R^2 = Me$	5	75

Scheme 1.19 Varying chain length and substitution α to the sulfone affects 1,5 vs. 1,6 C–H insertion.

Regioselective sultone formation has also been achieved by Du Bois and coworkers (Scheme 1.20). The strong preference for 1,6 C–H insertion was attributed to the similarity of the bond angles in the acyclic sulfonate and the cyclic sultone. The formation of a five-membered γ-sultone is inhibited as 1,5 C–H insertion would require an unfavorable C—S—O bond distortion [77].
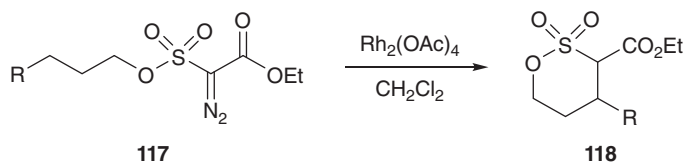
Scheme 1.20 Regioselective sultone formation.

The Taber group have synthesized cyclohexanones from α-diazo-β-aryl ketones with excellent regioselectivity by choosing electron-withdrawing aryl substituents α to the diazo moiety and electron donating substituents at the insertion site. The formation of a six-membered ring was in contrast to Taber's seminal work in the area. He rationalized this by illustrating how the electronic properties of donor/acceptor carbenoid, such as one derived from structure **119**, influences the selectivity for a different C—H bond than a carbenoid derived from an α-diazo-β-keto ester. Cyclohexanone **120** was synthesized in 99 : 1 selectivity over the corresponding cyclopentanone **121** (Scheme 1.21).
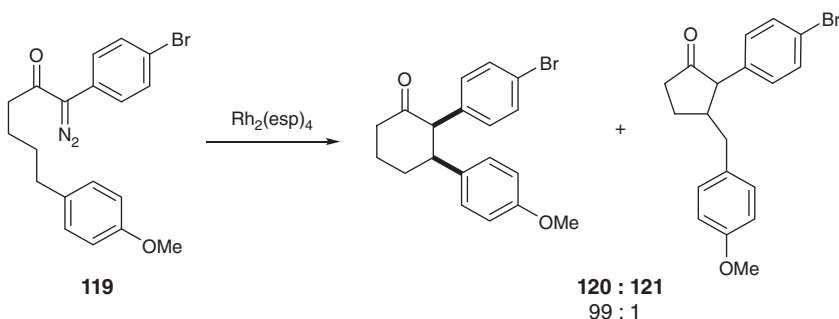

**Scheme 1.21** Regioselective cyclohexanone formation.

Du Bois and coworker have also reported stereoselective cyclohexanone formation as one of the key steps in their synthesis of the poison tetrodotoxin. The dirhodium catalyst employed for this transformation was $Rh_2(HNCOCPh_3)_4$ [78].

Maguire and coworkers have demonstrated the regioselective synthesis of cis thiopyran **124** with excellent enantioselectivity [30]. Interestingly this transformation is performed using a chiral copper-bisoxazoline catalyst complex. Surprisingly, when rhodium catalysts were applied to the similar substrate **122a**, the maximum asymmetric induction that could be achieved was 50% ee using $Rh_2(S\text{-PTTL})_4$. This could be increased to 90% ee when the ester moiety was replaced by a menthyl chiral auxiliary (Scheme 1.22) [79].

The reaction solvent has also been shown to influence the competition between 1,6 C–H insertion and β-hydride elimination. It has been reported that less polar solvents such as cyclohexane shift the reaction pathway toward 1,6 C–H insertion, while acetonitrile and tetrahydrofuran completely favor the β-hydride elimination process (Scheme 1.23) [80].
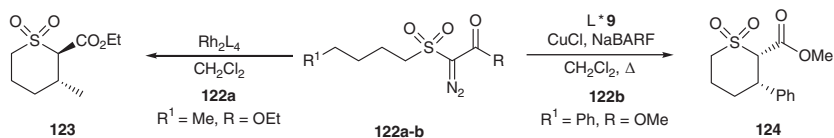
Scheme 1.22 Thiopyran synthesis in up to 98% ee can be achieved with copper-bisoxazoline catalytic system. Enantioselectivities are lower when rhodium catalysts are applied to similar α-diazocarbonyl substrates.
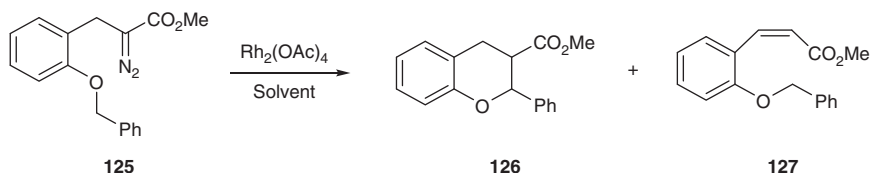

Entry	Solvent	Ratio 126 : 127
1	Cyclohexane	70 : 30
2	Benzene	54 : 46
3	Toluene	59 : 41
4	Dichloromethane	23 : 77
5	Dimethoxyethane	13 : 87
6	Tetrahydrofuran	0 : 100
7	Acetonitrile	0 : 100

Scheme 1.23 Solvent variation influences competition between 1,6 C–H insertion and β-hydride elimination.

1.5.3 Diastereoselectivity

1.5.3.1 Substrate Effects

Early studies by Taber and Ruckle [63, 81] and Doyle et al. [71] of $Rh_2(OAc)_4$-catalyzed cyclizations of disubstituted α-diazocarbonyl compounds noted the preferential formation of trans cyclopentanones and γ-lactones (Scheme 1.24).
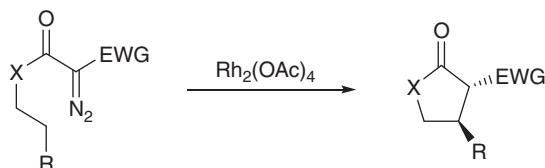
128a X = CH_2, EWG = CO_2R
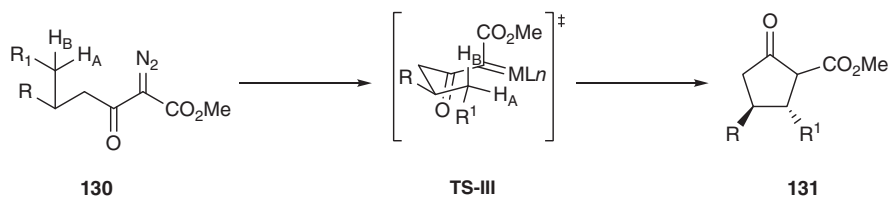**128b** X = O, EWG = COR   **129a,b**

Scheme 1.24 Preferential formation of trans cyclopentanones and γ-lactones as noted by Taber and Doyle.

In the C–H insertion reaction of **130**, the favored formation of trans products can be explained on the basis of a chair-like transition state (**TS-III**; Scheme 1.25), with insertion occurring into the C—H_A bond to give the trans diastereomer

Scheme 1.25 Synthesis of trans cyclopentanones proceeds through a proposed chair-like transition state.
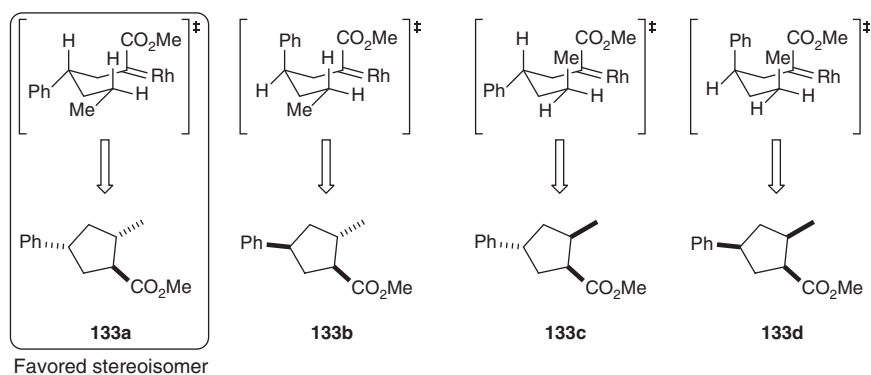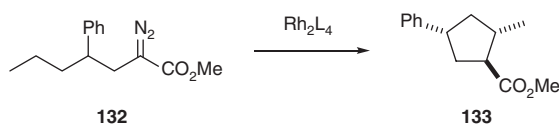

Figure 1.15 Four possible transition states of the carbenoid derived from α-diazocarbonyl compound **132** and the corresponding stereoisomers of cyclopentanone **133**.

of cyclopentanone **131**. Insertion into C—H_B bond to give the cis diastereomer would require R^1 in the less favorable axial position in the transition state [81].

Taber expanded this work by developing a computational model for predicting the diastereoselectivity of intramolecular C–H insertion reactions of α-diazoesters based on the cyclization of **132** (Figure 1.15) [18]. The relative transition state stabilities of the four possible transition states that would each lead to a different diastereomer of cyclopentanone **133** were analyzed. This model was then applied to α-diazo β-keto esters and accurately predicted the dominant stereoisomer formed. This study, together with another in-depth theoretical study by Nakamura and coworker [16], showed that the trans conformation is preferred in the cyclizations of α-diazoesters and α-diazo-β-keto esters due to the alkyl group at the insertion site occupying the equatorial position in the transition state. In contrast, the cis transition state suffers from 1,3-diaxial repulsion. The Nakamura calculations highlighted that a vinyl or phenyl group at the insertion site theoretically made the trans transition state less stable, but only trans products are observed experimentally.

1.5.3.2 Catalyst Effects

Doyle later reported excellent cis diastereoselectivity and high enantioinduction in the synthesis of bicyclic lactone **135** using the chiral rhodium catalyst $Rh_2(4S\text{-MACIM})_4$, while $Rh_2(5S\text{-MEOX})_4$ gave poor diastereocontrol when applied to the same system (Scheme 1.26) [82]. These examples are just some of the many reactions performed that highlighted the significant catalyst influence on the conformation of the reacting metal carbene and the resulting stereoselectivity [83–86].
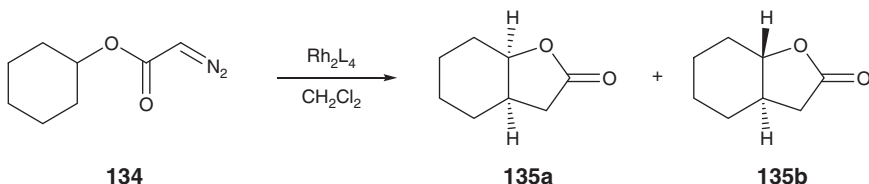
Entry	Rh_2L_4	%Yield 135a	%ee 135a	%Yield 135b	%ee 135b
1	$Rh_2(OAc)_4$	40	—	60	—
2	$Rh_2(4S\text{-MEOX})_4$	55	96	45	95
3	$Rh_2(5S\text{-MEPY})_4$	86	>99	14	93
4	$Rh_2(4S\text{-MACIM})_4$	99	97	1	65

Scheme 1.26 Ligands on the carboxamidate catalysts affect diastereocontrol.

1.5.4 Enantioselectivity

Recognizing the potential for asymmetric induction in intramolecular C–H insertion, Taber employed chiral auxiliaries to preferentially direct insertion into one face of the carbene. This was followed by the introduction of chiral ligands on the dirhodium scaffold leading to the first report of catalytic asymmetric C–H insertion of α-diazocarbonyl compounds by the McKervey group. To date, numerous studies have been reported investigating the influence of various chiral ligands and also substrate structure on the enantioselectivity of intramolecular C–H insertion reactions [1, 5, 6, 8].

Symmetry is a major factor in chiral catalysis as it reduces the number of transition states available during the stereodifferentiating step. The dirhodium paddlewheel structure achieves high symmetry through four identical ligands of low symmetry that surround a highly symmetric dirhodium core. Taking rhodium carboxylates as an example, the O–Rh–O plane can be viewed as a disc with an upper and a lower face, arbitrarily α and β (Figure 1.16). To induce asymmetry in a C–H insertion reaction, the ligands attached to the rhodium need to restrict the space above or below the O–Rh–O plane so that only one enantiotopic transition state is favored during the reaction, leading primarily to one enantiomer.

Depending on the orientation of these ligands toward the upper face or lower face of the O–Rh–O plane, dirhodium carboxylates can adopt multiple conformations. The symmetry of the complex is also affected by the inherent symmetry of the ligand. If ligands are C_1 symmetric, the most effective conformations for
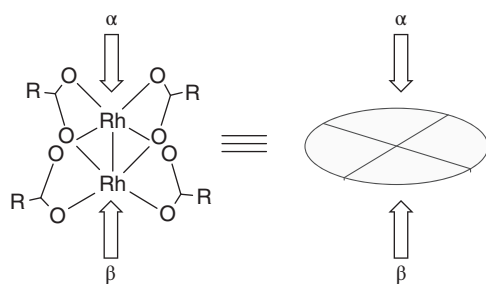
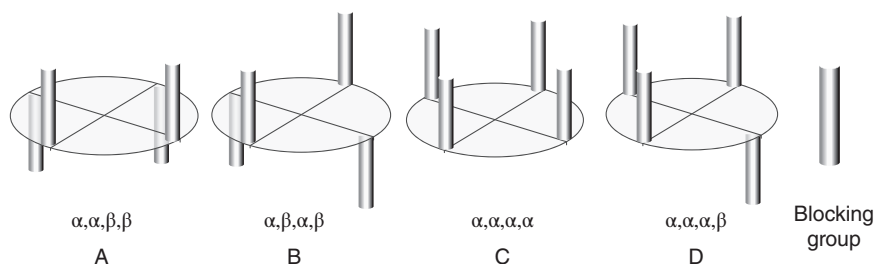**Figure 1.16** Viewing O–Rh–O plane as a disc with an α and β face.

Figure 1.17 Four possible conformations of C_1-symmetric ligands.

asymmetric catalysis are structures **A** (giving overall C_2 symmetry to the complex) and **B** (giving overall D_2 symmetry to the complex) as both faces of the plane are equivalent (Figure 1.17) [32]. Strong experimental evidence has also emerged for $Rh_2(S\text{-PTTL})_4$ and related catalysts (**29–40**) engaging in asymmetric cyclopropanation when ligands are in conformation **C**, the "all up" or crown conformation even though it had previously been dismissed as unable to catalyze reactions enantioselectively [87, 88]. While difficult to model experimentally, the catalyst ligands are thought to have more flexibility than once thought; this ligand flexibility is borne out by reports that describe enhancement of enantioselectivity with a change in solvent to a nonpolar solvent such as hexane or pentane [35].

If the carboxylate ligands possess C_2 symmetry, the overall symmetry of the catalyst can reach up to D_4, which is the optimal symmetry for these chiral dirhodium complexes as both faces of the O–Rh–O plane are equivalent (conformation **E**). D_2 symmetry can be achieved with two bridged C_2-symmetric ligands, such as bridged prolinates, providing a more rigid analog of the α,β,α,β conformation adopted by C_1-symmetric ligands (conformation **F**) (Figure 1.18).

The structures of chiral rhodium carboxamidates are more rigid in comparison and are limited to complexes of C_2 symmetry due to their preferred cis (2,2)
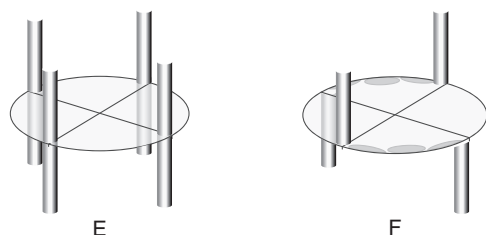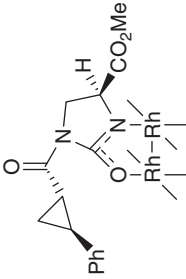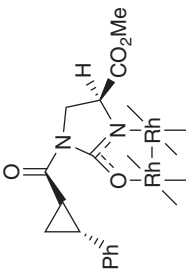
Figure 1.18 Possible conformations of C_2-symmetric ligands.
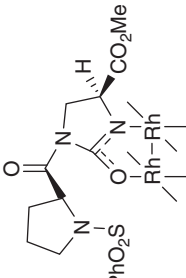
Entry	Rh$_2$L$_4$	%Yield 135a	%ee 135a	%Yield 135b	%ee 135b
1	136	99	97	1	—
2	137	80	72	20	13
3	138	97	>99	3	>99
4	139	98	74	2	33
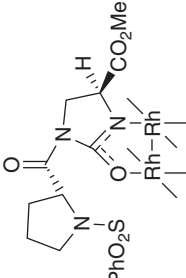
136 Rh$_2$(4S,2′S,3′S-MCPIM)$_4$

137 Rh$_2$(4S,2′R,3′R-MCPIM)$_4$

138 Rh$_2$(4S,2′S,-BSPIM)$_4$

139 Rh$_2$(4S,2′R,-BSPIM)$_4$

Figure 1.19 Different diastereomers of catalyst ligands lead to differing enantioselectivities.

conformation. They adopt the α,α,β,β conformation **A**. Although electron-dense carboxamidate ligands are less reactive than carboxylate ligands, they can be more selective in carbenoid-mediated reactions.

To explore the effect of changing the ligand orientation in space, two sets of diastereomeric catalysts, **136/137** and **138/139**, were used to cyclize the α-diazoacetate **134** (Scheme 1.26). Catalysts **136** and **138** led to excellent enantioselectivities, but there is a drop-off in asymmetric induction when the other isomers of the catalysts (**137**, **139**) are used. The different orientations of the ligands of different isomers lead to a conformation that is either "matched" or "mismatched" with the substrate structure [89] (Figure 1.19).

Bisoxazoline ligands have become some of the most widely used ligands in asymmetric catalysis due to the C_2-symmetric complexes that result when the ligands are coordinated to a metal such as copper. This C_2 symmetry results in equivalent structures upon rotation of the catalyst by 180°, meaning a reduction in the number of possible transition states and substrate approach trajectories during the reaction [90].

While catalyst symmetry is an important element in producing C–H insertion products with good enantiocontrol, so too is the electronic and steric nature of the ligands. Ligand-dependent enantioselectivity has been demonstrated in copper-bisoxazoline systems in studies reported by the Maguire group. Substrate **140** is just one example in a recent report of copper-catalyzed C–H insertion of α-diazocarbonyl compounds that were cyclized with five different commercially available bisoxazoline ligands. A wide variation in enantioselectivity was observed between the different ligands employed; the best asymmetric induction (87%) was achieved with the indane-derived bisoxazoline ligand (Scheme 1.27) [91].
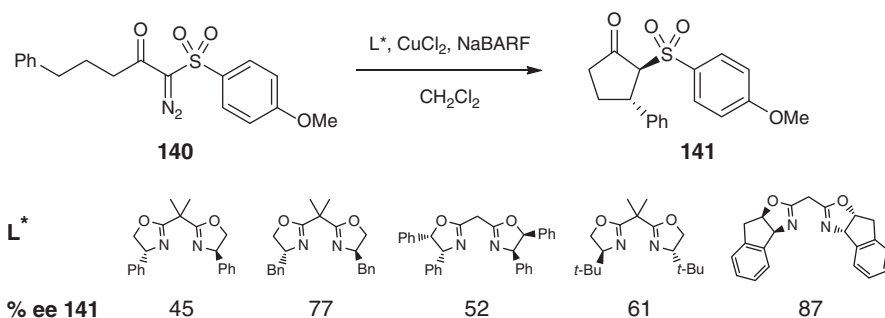
Scheme 1.27 Ligand-dependent enantioselectivity in copper-bisoxazoline-catalyzed C–H insertion.

In addition to catalyst effects on enantioselectivity, the substitution pattern of the α-diazocarbonyl substrate also has an important role to play. The Maguire group has also demonstrated how variation of both the substituent at the insertion site and the α-diazo substituent can have a dramatic effect on enantiocontrol of copper-catalyzed asymmetric C–H insertion.

To investigate substitution at the insertion site, a series of α-diazocarbonyl compounds were prepared and cyclized in the presence of a catalytic

system made up of a bisoxazoline ligand, $CuCl_2$, and an additive, sodium tetrakis(3,5-bis-(trifluoromethyl)phenyl)borate (NaBARF). It was found that, depending on the bisoxazoline ligand employed, variation of the electronic and steric properties at the insertion site could have a profound effect on enantioselectivity. In one example shown here (Scheme 1.28) using the diphenyl bisoxazoline ligand **13**, there was no enantioinduction with a methyl group at the insertion site, but moderate enantioinduction could be achieved with a phenyl group. This enantioselectivity dropped off again with a benzyl group. These experiments showed how substituents at the insertion site are very influential on the enantioselectivity of the reaction with a phenyl group proving optimal in this instance [29].
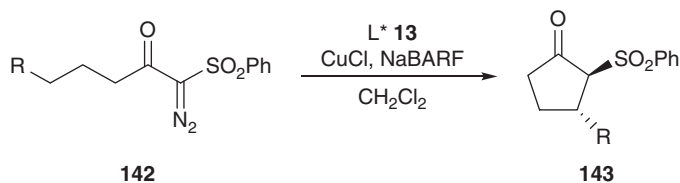
| Entry	142	R	%Yield 143	%ee 143
1	a	Me	75	0
2	b	Ph	82	58
3	c	Bn	46	0

Scheme 1.28 Varying the substitution pattern at the insertion site affects enantioselectivity.

Altering the substitution pattern α to the diazo moiety was also investigated. Initially various electron-withdrawing groups (sulfone, ester, ketone, phosphine oxide, and phosphonate) were examined for their impact on enantioselectivity (Scheme 1.29, Entries 1–5). The sulfone functionality is by far
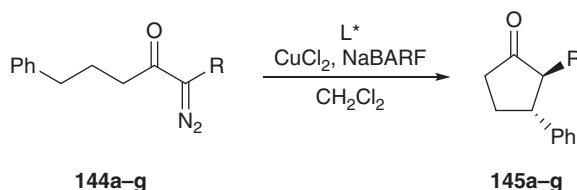
Entry	144	L*	R	%Yield 145	%ee 145
1	a	13	SO_2Ph	53	89
2	b	13	$CO_2CH(i\text{-}Pr)_2$	89	65
3	c	13	COPh	19	62
4	d	13	$PO(Ph)_2$	8	53
5	e	13	$PO(OMe)_2$	77	32
6	f	9	SO_2Me	49	8
7	a	9	SO_2Ph	69	50
8	g	9	$SO_2$1-Np	54	81

Scheme 1.29 Varying the electron-withdrawing group α to the diazo moiety affects enantioselectivity.

the superior electron-withdrawing group at the α-diazo site. The decreasing electron-withdrawing character of the other groups leads to reduced selectivity and longer reaction times [91, 92].

The steric and electronic impact at the α-diazo motif was also investigated with a series of alkyl and aryl sulfonyl substituents. A selection of results here (Scheme 1.29, Entries 6–8) highlights how the enantioselectivity increases with increasing steric bulk adjacent to the diazo. It was noted in this study that electronic effects had very little impact on the asymmetric induction [91]. In addition, different levels of asymmetric induction are observed when using two different ligands with the same substrate (Scheme 1.29, Entries 1 and 7). In this instance, the diphenyl bisoxazoline ligand affords excellent enantioselectivity in the cyclopentanone product, once again highlighting that when good enantiocontrol is desired as a key component of a chemical transformation, choosing the optimal catalyst and substrate structure for enantioselective C–H insertion requires careful consideration. Nonetheless, intramolecular C–H insertion has proven itself useful as a key step in the synthesis of numerous pharmaceutically relevant molecules, a few of which are noted here (Figure 1.20) [93–96].

1.6 Intermolecular C(sp^3)—H Bond Insertion

An intermolecular C–H insertion reaction consists of three components: a diazo compound, a substrate that may contain a range of functional groups, and a transition metal catalyst (Figure 1.21). This methodology has facilitated insertion into allylic, benzylic, and C(sp^3)—H bonds α to a heteroatom, as well as simple alkane substrates [97, 98]. The selectivity of intermolecular C–H insertion reactions is controlled by steric and electronic factors, with the ability to stabilize the buildup of positive charge during the transition state being key to its synthetic utility (Schemes 1.1 and 1.2). Intermolecular rhodium(II)-catalyzed reactions using acceptor/acceptor and acceptor-carbenoid complexes show limited selectivity due to the inability to stabilize the highly electrophilic carbenoid being generated. In order to achieve high levels of intermolecular selectivity at the desired C(sp^3)–H site on the substrate, a donor/acceptor metal carbenoid is most useful, as the donor group assists in the stabilization of the electron-deficient carbenoid [99].

Most research to date conducted in intermolecular C—C bond formation through C(sp^3)—H bond insertion by metal carbenoids is with the use of rhodium(II) catalysts. Accordingly, the reactivity and selectivity discussed in this section is primarily based on rhodium(II) catalysts unless otherwise stated.

1.6.1 Chemoselectivity

When carrying out an intramolecular C(sp^3)–H insertion, factors affecting chemoselectivity can be broken down into three sections: (i) diazo compounds, (ii) catalyst effects, and (iii) substrate functional groups.
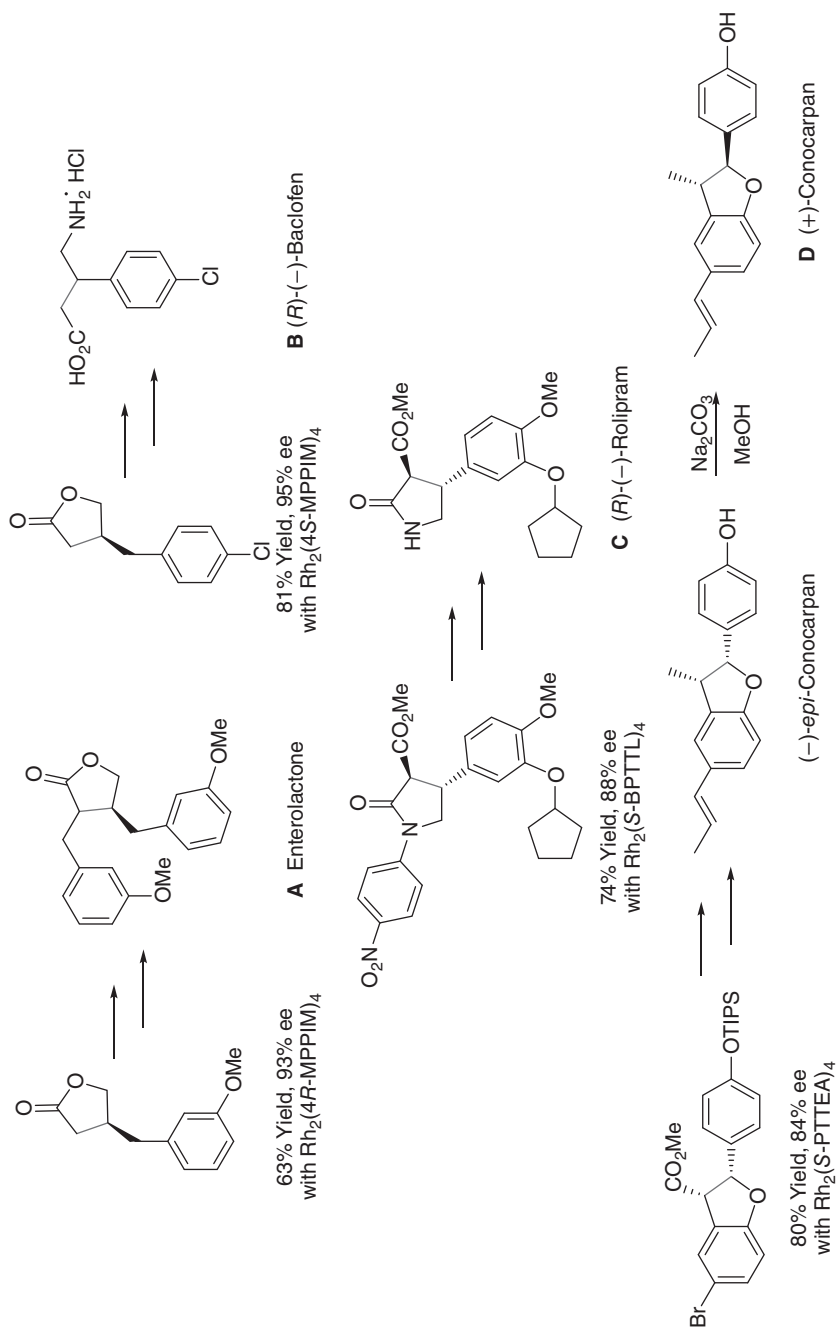
Figure 1.20 A selection of natural products that can be synthesized with high enantioselectivity using C–H insertion as a key step with the new C—C bond highlighted in light gray.
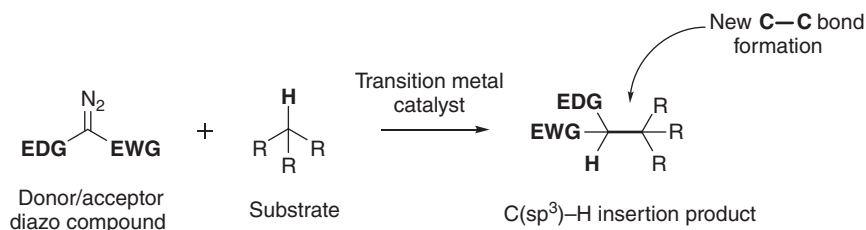
Figure 1.21 Intermolecular C–H insertion reaction between a donor/acceptor diazo compound and a substrate using a transition metal catalyst to form a new carbon–carbon bond.

1.6.1.1 Diazo Compounds

The need for a donor/acceptor-substituted diazo compound in intermolecular rhodium(II) catalytic systems to preferentially undergo $C(sp^3)$—H bond insertion over cyclopropanation is demonstrated using cyclohexene (**146**) and 1,4-cyclohexadiene (**150**) (Schemes 1.30 and 1.31) [100].
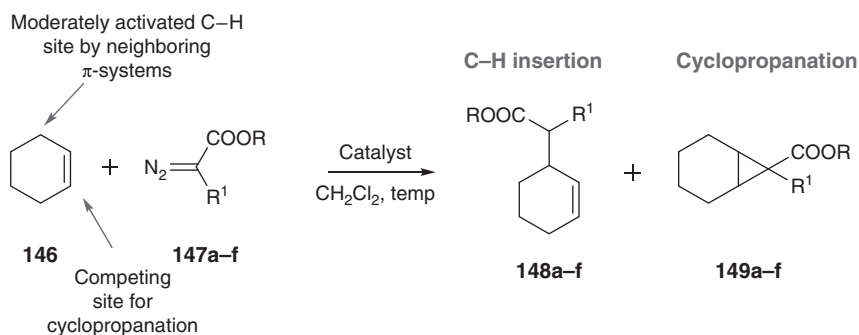
Entry	147	R	R^1	Catalyst	Ratio 148 : 149	%ee 148
1	a	Et	H	Rh$_2$(OAc)$_4$	20 : 80	—
2	b	DBMP^a	H	Rh$_2$(OAc)$_4$	67 : 33	—
3	c	Me	COOMe	Rh$_2$(OAc)$_4$	38 : 62	—
4	f	Me	Ph	Rh$_2$(OAc)$_4$	75 : 25	—
5	f	Me	Ph	Rh$_2$(2S-MEPY)$_4$	93 : 7	45
6	f	Me	Ph	Rh$_2$(S-PTPA)$_4$	50 : 50	53
7	f	Me	Ph	Rh$_2$(4S-DOSP)$_4$	80 : 20	75

^{a}DBMP = 2,6-di-*t*-butyl-4-methylphenyl.

Scheme 1.30 Competing C–H insertion and cyclopropanation of cyclohexene.

When cyclohexene is reacted with an acceptor substituted diazo compound, ethyl diazoacetate (**147a**), catalyzed by rhodium(II) acetate, cyclopropanation predominates over C–H insertion (80 : 20 ratio **149a** : **148a** (Scheme 1.30, Entry 1), and more noticeably when 1,4-cyclohexadiene is subjected to the same conditions, only the cyclopropanation product (**152a**) is isolated (Scheme 1.31,

Scheme showing highly activated C–H site by two neighboring π-systems; competing site for cyclopropanation (**150**) + diazo compound **147a–f** → C–H insertion product **151a–f** + Cyclopropanation product **152a–f**, with compound **153**.
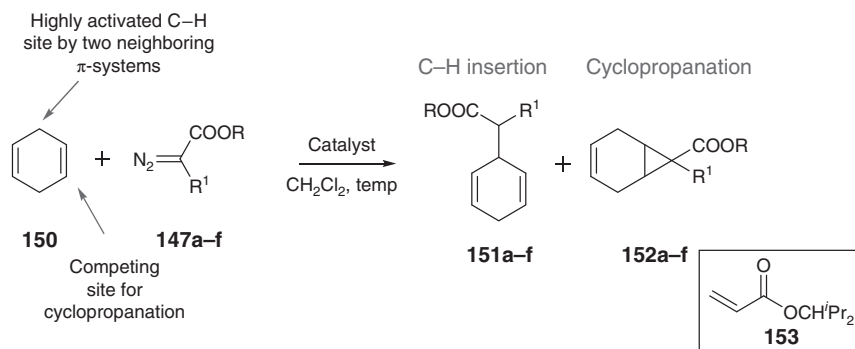
Entry	147	R	R^1	Catalyst	Temperature (°C)	Ratio 151 : 152	% ee 151
1	a	Et	H	Rh$_2$(OAc)$_4$	25	<2 : 98	—
2	c	Me	COOMe	Rh$_2$(OAc)$_4$	25	66 : 34	—
3^a	d	COOCH^{i}Pr$_2$	Me	Rh$_2$(S-TFPTTL)$_4$	0	72^b : —^{c}	82
4^a	e	COOCH^{i}Pr$_2$	Et	Rh$_2$(S-TFPTTL)$_4$	−60	—^{d} : —	—
5	f	Me	Ph	Rh$_2$(OAc)$_4$	25	>98 : 2	—
6	f	Me	Ph	Rh$_2$(2S-MEPY)$_4$	25	>98 : 2	4
7	f	Me	Ph	Rh$_2$(S-PTPA)$_4$	25	>98 : 2	40
8	f	Me	Ph	Rh$_2$(4S-DOSP)$_4$	25	>98 : 2	65
9	f	Me	Ph	Ir(III)-salen (**57**)	0	>95 : 5	94
10	f	Me	Ph	Ir(III)-porphyrin (**59**)	−40	>99 : —^{c}	95
11	f	Me	Ph	Ir(III)-bis(oxz) (**58**)	rt	>99 : —^{c}	97

^{a}2,2-Dimethylbutane was the reaction solvent used. ^{b}Isolated yield.
^{c}Cyclopropanation product was not observed in reaction mixture.
^{d}No C–H insertion product was observed but only the 1,2-hydride shift alkene (**153**).

Scheme 1.31 Competing C–H insertion and cyclopropanation of 1,4-cyclohexadiene.

Entry 1). Improvements in C–H insertion selectivity can be obtained by the use of a bulky ester, 2,6-di-*t*-butyl-4-methylphenyl (DBMP), ester (**147b**), where cyclopropanation is suppressed to an extent (Scheme 1.30, Entry 2).

If an acceptor/acceptor-substituted diazo compound, such as dimethyl malonate **147c** is used (Scheme 1.30, Entry 3 and Scheme 1.31, Entry 2), poor selectivity for C–H insertion is also achieved. Recently, it has been shown that the use of an α-alkyl-α-diazoester (**147d**) with 1,4-cyclohexadiene gives the corresponding C–H insertion product with modest yields and good enantioselectivity (Scheme 1.31, Entry 3) [101]. However, when the α-alkyl substituent is changed to ethyl (**147e**), no C–H insertion product is observed, and only the 1,2-hydride shift product (**153**) is isolated (Scheme 1.31, Entry 4). Achiral copper catalysts were also tested, but resulted only in high levels of cyclopropanation.

Substrate design showed that the donor/acceptor substituted diazo compound **147f** delivers selectively **151** regardless of the catalyst used (Scheme 1.31, Entries 5–11).

A second example of a donor/acceptor-substituted diazo compound is vinyl-diazoacetate (**154**), which undergoes selective C–H insertion into cyclohexane
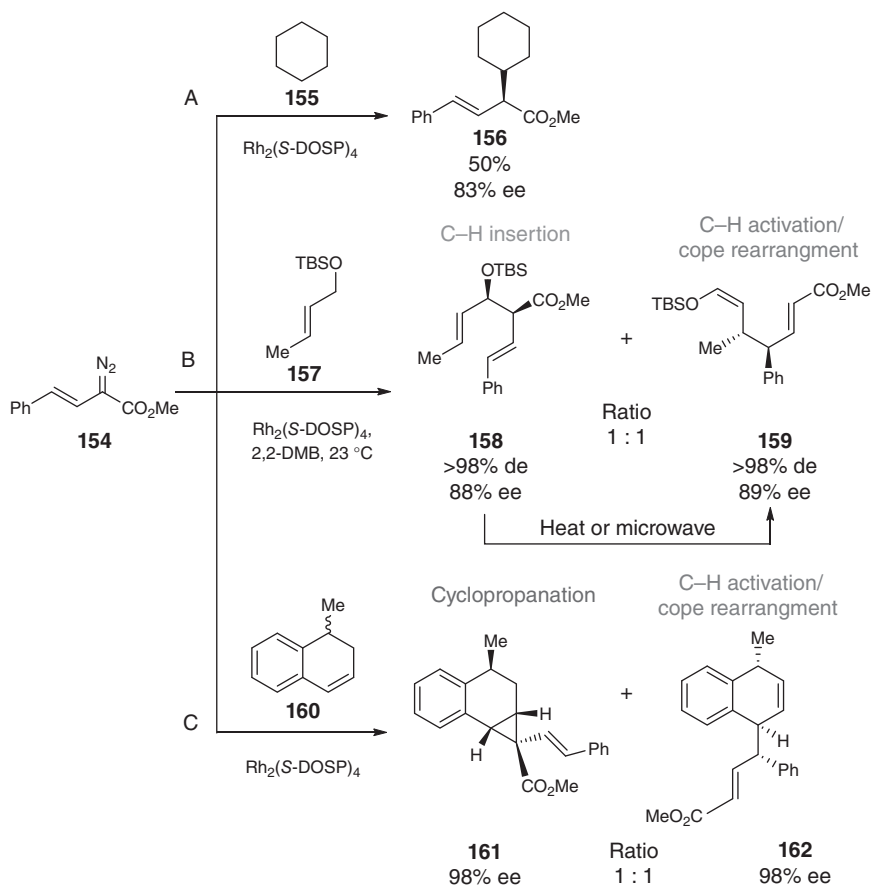
Scheme 1.32 Donor/acceptor diazo compound, vinyldiazoacetate, undergoes a range of competing reaction pathways.

(**155**) using $Rh_2(S\text{-DOSP})_4$, with moderate yield (50%) and high levels of enantioselectivity (83% ee) (A, Scheme 1.32) [36]. However, vinyldiazoacetates are relatively unstable, and their use has been limited due to spontaneous [1,5]-cyclization to yield pyrazoles [102]. In certain $Rh_2(S\text{-DOSP})_4$ catalyzed intermolecular C–H insertion reactions where acyclic or cyclic substrates containing allylic $C(sp^3)$—H bonds were investigated, vinyldiazoacetate (**154**) undergoes highly diastereoselective and enantioselective C–H insertion (**158**), cyclopropanation (**161**), and C–H activation/Cope rearrangement (**159** and **162**), with poor chemoselectivity for C–H insertion observed overall (B and C, Scheme 1.32) [36, 103, 104].

1.6.1.2 Catalyst Effects

When cyclohexene and the methyl phenyldiazoacetate (**147f**) are reacted with a range of rhodium(II) catalysts, moderate to high selectivity toward allylic $C(sp^3)$–H insertion over cyclopropanation is observed at the moderately activated secondary site (Scheme 1.30, Entries 4–7). The highest level

of chemoselectivity is observed with a rhodium(II) carboxamidate catalyst, $Rh_2(2S\text{-MEPY})_4$, although with the lowest level of enantioselectivity (45% ee) (Scheme 1.30, Entry 5). These catalysts display varying steric and electronic properties, with a combination of both factors proposed to influence selectivity at the moderately activated cyclic C(sp³)–H site.

Similarly, chiral iridium complexes can be used to carry out the same intermolecular C–H insertion reaction with 1,4-cyclohexadiene (**150**) (Scheme 1.31, Entries 9–11) [51–53]. Insertion into the C(sp³)—H bond predominates over cyclopropanation, regardless of the ligands. At low temperatures (Entries 9 and 10), high yields and enantioselectivity are observed. The iridium(III)-bis(oxazolinyl)phenyl catalyst (**58**) appears to be more advantageous, with good yields and the highest level of enantioselectivity even at room temperature (Scheme 1.31, Entry 11).

The chemoselectivity for C–H insertion over cyclopropanation of an allylic substrate can be controlled by the catalyst [38, 105]. $Rh_2(esp)_4$ is found to favor cyclopropanation in the reaction between trans-anethole (**163**) and aryldiazoacetate (**164**), with $Rh_2(R\text{-DOSP})_4$ achieving moderate levels of C–H insertion (Scheme 1.33, Entries 1 and 2). Interestingly, when using a more sterically congested catalyst system such as $Rh_2(TPA)_4$ or $Rh_2(R\text{-BPCP})_4$, C–H insertion is predominantly observed (Scheme 1.33, Entries 3 and 4).
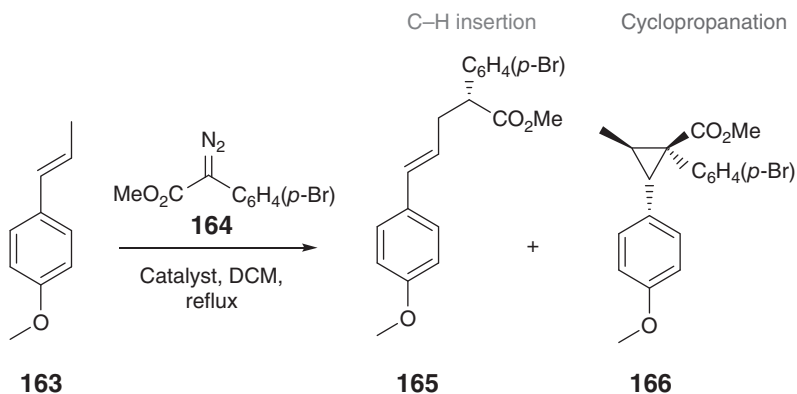
Entry	Catalyst	Ratio 165 : 166	% ee 165
1	$Rh_2(esp)_2$	1 : >15	—
2	$Rh_2(R\text{-DOSP})_4$	5 : 1	76
3	$Rh_2(TPA)_4$	>15 : 1	—
4	$Rh_2(R\text{-BPCP})_4$	16 : 1	88

**Scheme 1.33** Intermolecular chemoselectivity varies in certain cases with more sterically congested rhodium(II) catalysts.

1.6.1.3 Substrate Functional Groups

The chemoselectivity in allylic systems is influenced by steric effects. Monosubstituted and 1,1-disubstituted alkene substrates lead preferentially to cyclopropanation, while enhanced steric demand in trisubstituted alkenes favors C–H

insertion [105, 106]. Electronic effects of the aryl ring on substituted trans styrene substrates can also have an effect on the product distribution between insertion and cyclopropanation. Electron-poor alkenes are highly selective toward C–H insertion, while electron-rich alkenes predominantly undergo cyclopropanation.

Another factor that may have to be taken into consideration on the substrate undergoing C–H insertion is the presence of a heteroatom. The Lewis base nature of compounds such as ethers, sulfides, amines, and carbonyl compounds means they are prone to ylide formation and subsequent rearrangement, which is very common with alkyl and aryldiazoacetates. It has been shown that tetrahydrofuran (**167**) can undergo selective $C(sp^3)$–H insertion α to oxygen (**168a** and **168b**) in moderate yields using rhodium and copper (Scheme 1.34, Entries 1–3) [107, 108]. The preference for $C(sp^3)$–H insertion in this reaction is also observed with the use of iridium-based chiral catalysts at low temperatures (Scheme 1.34, Entries 4–7) [51, 53].
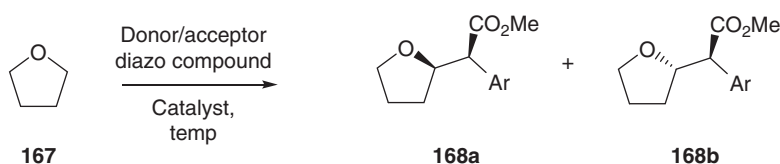
Entry	Diazo	Catalyst	Tempe-rature (°C)	Yield (%)	Ratio 168a : 168b	%ee 168a	%ee 168b
1	**147f**	$Rh_2(S\text{-}DOSP)_4$	−50	67	2.8 : 1	97	—
2	**147f**	$Cu(OTf)_2 \cdot L^*$ **9**	Reflux	48[a]	1.7 : 1	59	40
3	**147f**	$Cu(OTf)_2 \cdot$ immobilised L* **9**	Reflux	59[a]	3.5 : 1	88	46
4	**147f**	Ir(III)-salen (**56**)	−50	75	13 : 1	95	—
5	**147f**	Ir(III)-porphyrin (**59**)	−40	82	1 : 10	—	90
6	**164**	Ir(III)-salen (**56**)	−50	76	>20 : 1	93	—
7	**164**	Ir(III)-porphyrin (**59**)	−40	96	1 : >20	—	97

[a]Conversion to C–H insertion product observed.

Scheme 1.34 Intermolecular C–H insertion of THF.

Further examples of substrates containing heteroatoms include allyl ethers and silyl allyl ethers, where both the cyclopropanation and C–H insertion product are formed, in contrast with allyl acetate in which only the cyclopropanation product is formed [109]. Examples of C–H insertion α to a protected nitrogen are also known (Figure 1.23 and Scheme 1.39).

1.6.2 Regioselectivity

1.6.2.1 Substrate Effects

There are three types of sites for $C(sp^3)$–H insertion: primary, secondary, and tertiary (Figure 1.22a). The favorability of a site toward intermolecular function-alization is dependent on the ability to stabilize the buildup of positive charge during the transition state, which is more easily achievable at a tertiary site, rather
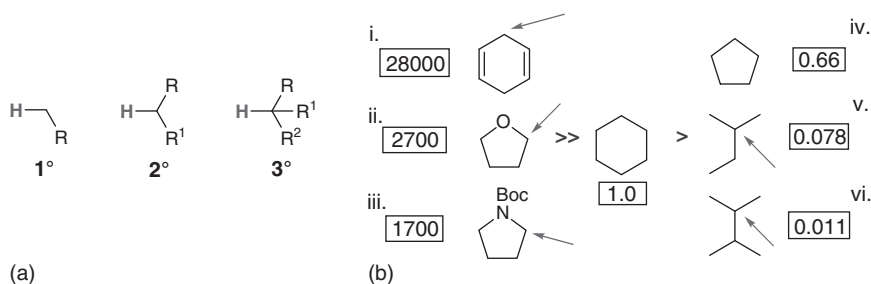
Figure 1.22 (a) Primary, secondary, and tertiary $C(sp^3)$–H site. (b) Relative rates of C–H insertion using aryldiazoacetate.

than a secondary site, and less so for a primary site. However, from the perspective of accessibility, reactions at the least sterically hindered primary site are often favored over a secondary or tertiary site. Insertion at secondary $C(sp^3)$–H sites is commonly seen as a compromise between electronic stabilization and steric effects [110].

Davies and coworkers investigated the factors affecting intermolecular C–H insertion regioselectivity using rhodium(II) catalysts [20]. This work highlighted how electronic and steric effects play an important role in intermolecular C–H insertion compared with intramolecular C–H insertion, where five- or six-membered ring formation dominates regioselectivity.

The reactivity of $C(sp^3)$—H bonds were compared with the C—H bonds in cyclohexane, which was given a relative reactivity of 1 (Figure 1.22b). 1,4-Cyclohexadiene (Figure 1.22b, i) is found to be 28 000 times more reactive toward C–H insertion, with C–H sites α to a heteroatom such as oxygen and nitrogen, 2700 and 1700 times more reactive, respectively (Figure 1.22b, ii and iii). Electronic effects have a major impact on C–H insertion in the first three cases (Figure 1.22b, i–iii); however in the second three cases (Figure 1.22b, iv–vi), steric effects can be seen to play a role. While insertion at a tertiary bond would be more electronically favored over a secondary bond, in practice, 2-methylbutane (v) and 2,3-dimethylbutane (vi) are found to undergo C–H insertion 10 and 100 times more slowly, respectively, than cyclohexane. Similarly, $C(sp^3)$–H insertion at relatively activated benzylic and acyclic allylic positions is also favored.

Insertion at a primary $C(sp^3)$—H bond is challenging except in cases where it is activated, for example, being α to a nitrogen or oxygen. It is interesting to note here that C—H bonds β to oxygen have been shown not to undergo C–H insertion, possibly due to inductively destabilizing the buildup of positive charge during the transition state (Scheme 1.35) [107].
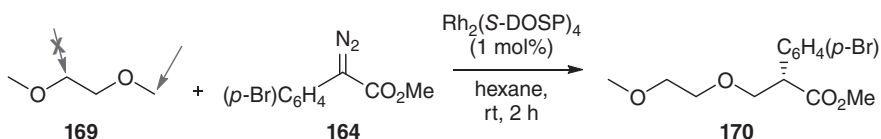
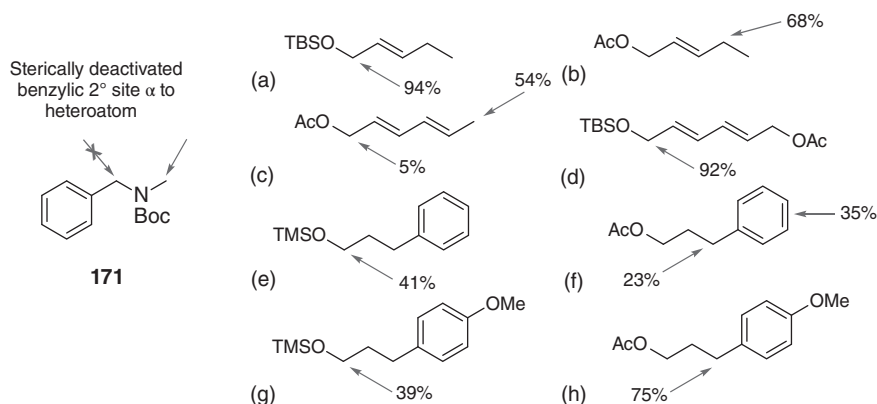**Scheme 1.35** C–H insertion favored at sites α to oxygen but not β.

Figure 1.23 Steric factors affecting C–H insertion and varying effect of different alcohol protecting groups on intermolecular C–H insertion with aryldiazoacetate.

The reactivity patterns that would be anticipated by electronic effects are frequently moderated by steric effects. For instance, a secondary benzylic site α to a heteroatom (**171**) is a very favorable site for insertion; however, the presence of a Boc protecting group sterically blocks the electronically favored secondary position, and C–H insertion occurs at the primary position (Figure 1.23) [111].

An overview of how protecting groups affect C–H insertion electronically is illustrated by the reactions of protected alcohols [109]. The electron-rich TBS group is able to stabilize the buildup of positive charge, and as a result, high yielding C–H insertion at a secondary site α to the oxygen is observed (Figure 1.23a). With an electron-withdrawing acetate protecting group, the α position is deactivated, and minimal C–H insertion is observed at this site, with C–H insertion occurring predominantly at the alternative allylic position (Figure 1.23b). C–H insertion across a range of protected alcohols can be seen to occur at the most electron-rich site (Figure 1.23).

1.6.2.2 Catalyst Effects

It has been shown that site selectivity for the primary C—H bond with benzylic, methoxy, and allylic C—H bonds can be enhanced by the use of a catalyst with sterically demanding ligands, $Rh_2(R\text{-BPCP})_4$, in place of the widely employed catalyst, $Rh_2(R\text{-DOSP})_4$ (Scheme 1.36) [38]. 4-Isopentyltoluene (**172**) contains a primary and a secondary benzylic site that undergo C–H insertion at a comparable extent with aryldiazoacetate **164** using $Rh_2(R\text{-DOSP})_4$ or $Rh_2(S\text{-PTAD})_4$ (Scheme 1.36, Entries 1 and 2). When the sterically demanding catalyst $Rh_2(R\text{-BPCP})_4$ is used on the same substrate, regioselectivity predominantly shifts to the primary site (>20 : 1) (Scheme 1.36, Entry 3). The same high levels of regioselectivity and enantioselectivity are observed with a range of aromatic substrates. It is interesting to note here that no reaction is observed at the tertiary C–H site of 4-isopentyltoluene (**172**).

The selectivity of $Rh_2(R\text{-BPCP})_4$ toward primary C–H insertion also applies to allylic substrates [38]. $Rh_2(R\text{-DOSP})_4$ favored functionalization at the tertiary position, which electronically stabilizes the buildup of positive charge, while
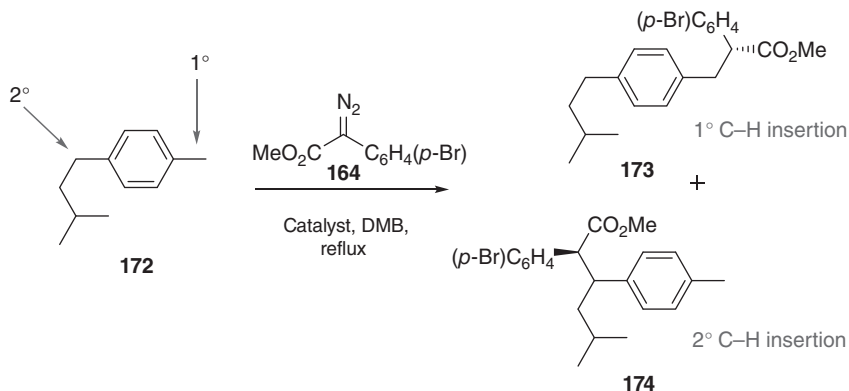
Entry	Catalyst	Ratio 173:174	%Yield[a] 173	%ee 173
1	$Rh_2(R\text{-DOSP})_4$	1:1.7	70	77
2	$Rh_2(S\text{-PTAD})_4$	1.1:1	73	70
3	$Rh_2(R\text{-BPCP})_4$	>20:1	90	94

[a] The yields of Entries 1 and 2 are the combined yields of **173** and **174**.

Scheme 1.36 Impact of rhodium(II) carboxylate ligands on regioselectivity of C–H insertion.

$Rh_2(R\text{-BPCP})_4$ showed a strong bias for insertion at the easily accessible primary position. Even though it has been demonstrated that regioselective C–H insertion at secondary and tertiary sites can be achieved using $Rh_2(R\text{-DOSP})_4$ and primary sites can be functionalized using $Rh_2(R\text{-BPCP})_4$, the rationale to explain these results is not yet fully understood. The bulky nature of the ligands on rhodium(II) catalysts facilitating the intermolecular insertion at primary C–H sites is not the only contributing factor as a new sterically demanding triarylcyclopropanecarboxylate catalyst, $Rh_2[R\text{-3,5-di}(p\text{-}^tBuC_6H_4)TPCP]_4$, can exclusively access a secondary position in simple alkane substrates with high diastereoselectivity and enantioselectivity, instead of the least sterically hindered primary position available for insertion [98].

1.6.2.3 Diazo Compound Effects
Changing from the methyl aryldiazoacetate to the 2,2,2-trichloroethyl (TCE) aryldiazoacetate ester affords higher regio- and enantioselectivity in certain cases [112]. A higher level of regioselectivity is observed at the primary position over the secondary benzylic position in 4-ethyltoluene (**175**) when the trichloroethyl ester is used as the coupling partner instead of the methyl ester with $Rh_2(R\text{-BPCP})_4$ (Scheme 1.37).

1.6.3 Diastereoselectivity

1.6.3.1 Substrate Effects
Controlling diastereoselectivity is one of the most challenging aspects in intermolecular C(sp³)–H insertion as it is strongly substrate and catalyst dependent. The mechanism of C(sp³)–H insertion has been examined in recent
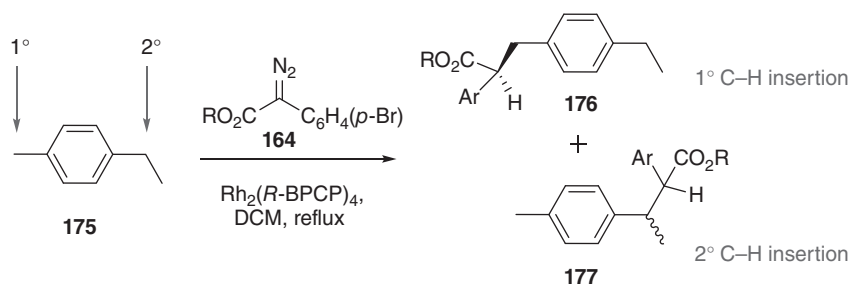
Entry	R	176 : 177	%Yield 176	%ee 176
1	Me	5 : 1	74	92
2	CH$_2$CCl$_3$	13 : 1	75	99

Scheme 1.37 2,2,2-Trichloroethyl aryldiazoacetate achieves higher regio- and enantioselectivity over methyl aryldiazoacetate.

computational studies; it is assumed that relatively activated C(sp^3)—H bonds approach perpendicular to the metal carbenoid. It is believed that during this approach, the substrate substituents are orientated in the least sterically hindered manner. The directional approach taken by the substrate substituents to the metal carbenoid is determined by the steric environment of the catalyst. The hypothesised D_2 symmetrical Rh$_2$(S-DOSP)$_4$ consists of a dirhodium paddlewheel (represented by a disc) and its respective ligands in an α-β-α-β arrangement (represented by a wedge) (Figure 1.24) [110]. The ester group on the metal carbenoid is sterically demanding as it is perpendicular to the plane of the metal carbenoid, and as a result the smallest substituent (S) is positioned between the ester and the rhodium catalyst ligand, the less sterically crowded position. The largest substituent (L) positions itself the furthest away from the rhodium(II) catalyst paddlewheel and the catalyst ligands, pointing upward, with the second most sterically demanding substituent (M) pointing away from the catalyst ligands but toward the dirhodium paddlewheel as a result. This model can therefore be used in an attempt to predict the stereochemical outcome of intermolecular C–H insertion reactions.

A large body of experimental research in intermolecular C–H insertion supports the above rationale of diastereocontrol (Figure 1.24) [110]. For example, when the medium and small substituents are methylene and hydrogen, respectively, the differentiation is small, and as a result, poor diastereoselectivity is observed (Figure 1.24a). However, high diastereocontrol is observed in cases where the difference in size is large (Figure 1.24b). A similar result can be observed when tetrahydrofuran is compared with *N*-Boc pyrrolidine. On the tetrahydrofuran group, there is little difference between the –CH$_2$– and the –O– substituents, yielding moderate diastereocontrol (Figure 1.24c); however, with the *N*-Boc pyrrolidine ring, there is a significant size differentiation between the *N*-Boc protecting group and the –CH$_2$–, affording high levels of stereocontrol (Figure 1.24d). Modest diastereocontrol is observed when using indane (Figure 1.24e); however, when the ring was changed to tetrahydronaphthalene,
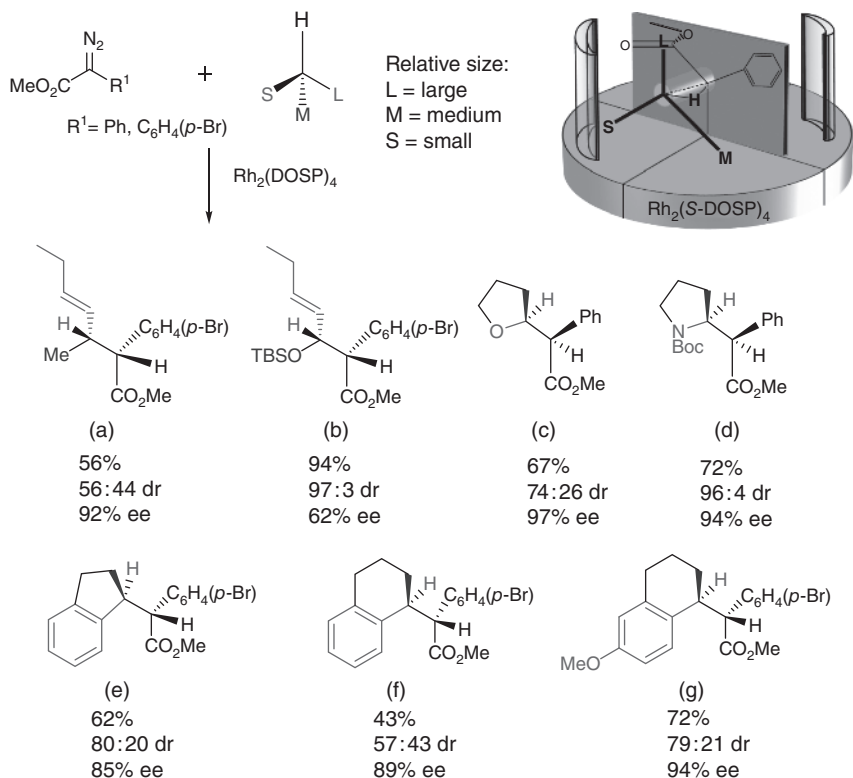
Figure 1.24 Predicting diastereocontrol by differentiating between the relative size of substituents. Source: Davies and Morton [110]. Reproduced with permission of John Wiley & Sons.

poor diastereocontrol resulted (Figure 1.24f). The change between a five- and six-membered ring in these specific cases leads to decreased diastereocontrol, but the presence of an electron-donating group improves diastereocontrol (Figure 1.24g).

Another good example of substituent-dependent diastereocontrol, and how it can be controlled in a predictable manner, is seen in Scheme 1.38 [113]. When R = H, cyclopropanation dominates over C—H insertion; however, 15% yield of the C—H insertion product was isolated with poor diastereocontrol (52 : 48 dr) and 93% ee (Scheme 1.38, Entry 1). The poor stereocontrol observed is attributable to the marginal differentiation between the medium and large substituent observed during the substrate approach to the metal carbenoid. When 1-(trimethylsilyl)cyclohexene is used, an increase in diastereoselectivity is observed due to the more sterically demanding TMS group, with the catalyst able to favor one substrate approach over the other (Scheme 1.38, Entry 2). In order to achieve high levels of diastereoselectivity, the extremely bulky *tert*-butyldiphenylsilyl (R = TBDPS) substituent is required, affording the expected product with 94 : 6 dr, a yield of 64%, and 95% ee (Scheme 1.38, Entry 3).

Scheme 1.38 High levels of diastereocontrol with increased steric hindrance.
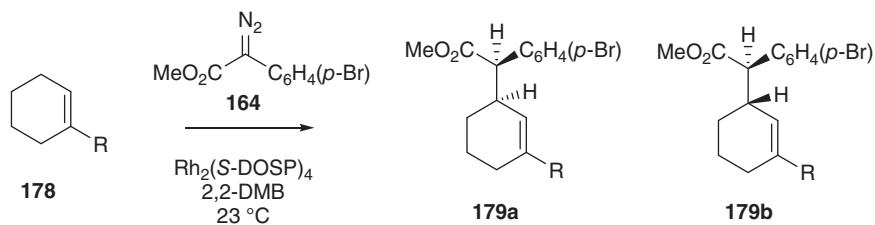
Entry	R	%Yield 179a	dr 179a : 179b	%ee 179a
1	H	15	52 : 48	93
2	TMS	48	70 : 30	88
3	TBDPS	64	94 : 6	95

1.6.3.2 Catalyst Effects

The catalyst can be seen to have a major impact on diastereocontrol, for example, as with *N*-Boc piperidine [31]. In an attempt to increase the diastereoselectivity of C–H insertion into the *N*-Boc protected piperidine ring, the reaction was examined with a number of catalysts. A chiral carboxamidate catalyst, $Rh_2(5R\text{-MEPY})$, exhibited the highest degree of diastereoselectivity (97 : 3 dr) with a modest enantioselectivity of 69% ee (Scheme 1.39, Entry 5). The $Rh_2(S\text{-DOSP})_4$ catalyst that produces a high level of diastereoselectivity for the pyrrolidine ring (96 : 4 dr) (Figure 1.24d) gave poor selectivity when reacted with piperidine (50 : 50 dr) (Scheme 1.39, Entry 1). Another rhodium(II) carboxylate catalyst examined, $Rh_2(S\text{-biDOSP})_4$, induced higher diastereoselectivity (71 : 29 dr), but the major diastereomer **181a** shows a moderate enantiopurity of 86% ee (Scheme 1.39). A copper Schiff base catalyst (Scheme 1.39, Entry 6) performed
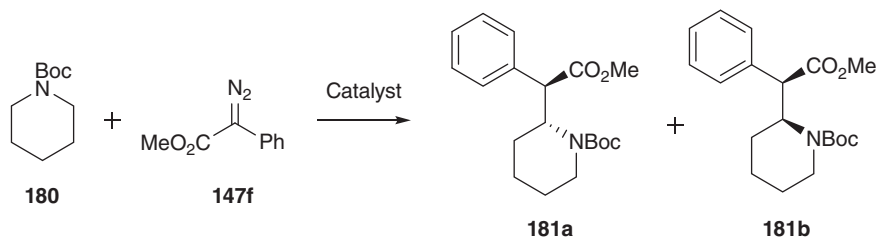
Entry	Catalyst	dr 181a : 181b	%ee 181a
1	$Rh_2(S\text{-DOSP})_4$	50 : 50	25
2	$Rh_2(S\text{-biDOSP})_4$	71 : 29	86
3	$Rh_2(4S\text{-MPPIM})_4$	55 : 45	16
4	$Rh_2(4S\text{-IBAZ})_4$	93 : 7	26
5	$Rh_2(5R\text{-MEPY})_4$	97 : 3	69
6	$(CuOTf)_2 \cdot L*$ **16**	70 : 30	18

Scheme 1.39 Catalyst effect on six-membered *N*-Boc protected piperidine.

poorly on the same system, generating only moderate diastereocontrol (70 : 30) and poor enantioselectivity (18% ee).

1.6.4 Enantioselectivity

Intermolecular $C(sp^3)$–H insertion of metal carbenoids derived from aryldiazoacetates has been shown to be a highly enantioselective process, specifically with the use of chiral rhodium(II) catalysts and, in recent times, iridium(III) complexes. Even though there are challenges in controlling chemo-, regio-, and diastereoselectivity, moderate to high levels of enantiopurity can generally be achieved.

Many examples of enantiocontrol at primary, secondary, and tertiary $C(sp^3)$—H bonds have been observed while achieving moderate to high yields (Figure 1.25a–f) [36, 38, 42, 112–115]. The substrates for which high levels of enantiopurity can be achieved range from the simple cyclohexane to more challenging C–H positions, e.g. allylic or α to a heteroatom. Since the recent development of the TCE aryldiazoacetates, further improvements in yields and enantioselectivity of reactions at methyl ether groups have also been achieved with C–H insertion occurring at the primary position α to the oxygen (Figure 1.25g,h) [38].

While enantioselectivity with chiral rhodium(II) catalysts can sometimes be improved at lower temperature and in hydrocarbon solvents, it is interesting to take note of the chemo- and regioselective outcome by various catalysts on the reaction. In Scheme 1.36, the highest level of enantiopurity was obtained for the formation of **173** when catalyst favoring insertion at the primary C—H bond is used. Similarly, the greatest ee (88%) in the formation of **165** is seen while using $Rh_2(R\text{-BPCP})_4$ (Scheme 1.33), which is the most selective for C–H insertion over
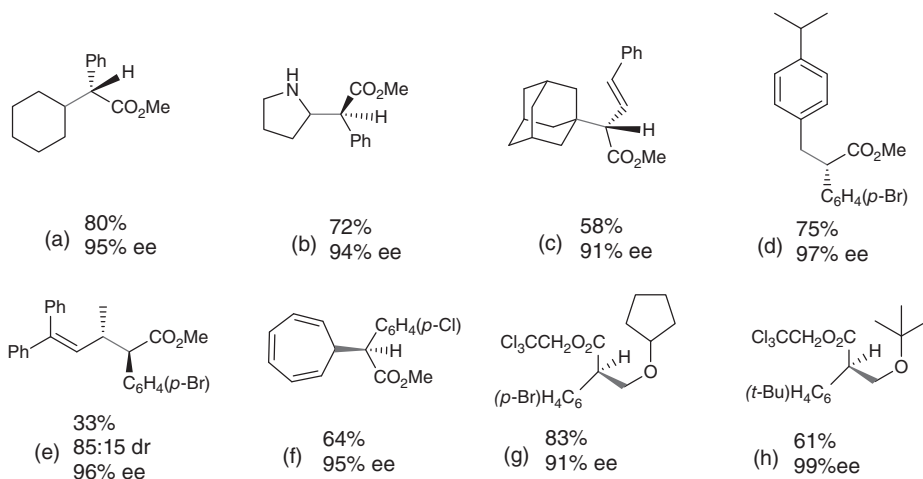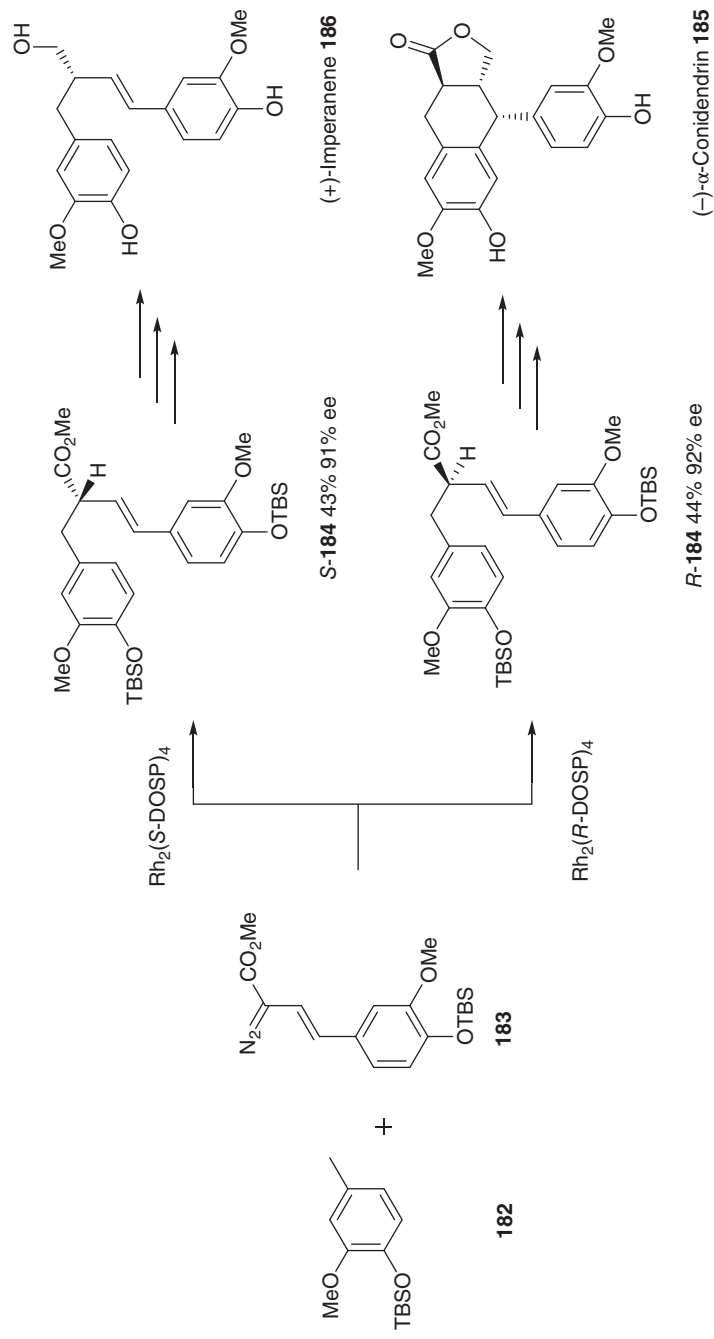

Figure 1.25 Examples of high enantiopure yielding C–H insertion products using rhodium catalysts. New C—C bond highlighted in light gray.

S-184 43% 91% ee

(+)-Imperanene 186

R-184 44% 92% ee

(−)-α-Conidendrin 185

Rh$_2$(S-DOSP)$_4$

Rh$_2$(R-DOSP)$_4$

183

182

+

Scheme 1.40 Synthesis of enantiopure (−)-α-conidendrin and (+)-imperanene.

cyclopropanation. A highly chemo- and regioselective catalyst is important at times for optimal enantiopurity levels.

There are few examples of vinyldiazoacetates producing high levels of enantioselectivity during intermolecular $C(sp^3)$–H insertion. However one of the key applications concerns the synthesis of chiral ligands for dirhodium(II) carboxylate catalysts. An adamantane tertiary site undergoes C–H insertion with methyl vinyldiazoacetate furnishing the rhodium(II) catalyst precursor with 91% ee (Figure 1.25c). This enabled the synthesis of $Rh_2(S\text{-PTAD})_4$ (**35**) [116]. The versatility of vinyldiazoacetates in enantioselective synthesis is also palpable in accessing (−)-α-conidendrin (**185**) and (+)-imperanene (**186**; Scheme 1.40) [117]. $Rh_2(R\text{-DOSP})_4$ was used to access one enantiomer (91% ee) via C–H insertion on an electron-rich benzylic primary C–H site, while $Rh_2(S\text{-DOSP})_4$ was used to synthesize the opposite enantiomer (92% ee). This highlights the importance of the availability of both enantiomers of the catalyst in accessing natural products (Scheme 1.40).

Other examples of natural product synthesis that have taken advantage of the high enantioselectivity of intermolecular C–H insertion using both enantiomers of $Rh_2(DOSP)_4$ catalysts include the antidepressant agent venlafaxine [118] and the antisickling agent (+)-cetiedil [119].

1.7 Conclusion

Overall, carbenoid-mediated C–H insertion is a very powerful transformation enabling functionalization of an unactivated C—H bond under mild, neutral conditions. Catalyst developments over the past three decades have enabled regio-, diastereo-, and enantioselectivity in both intra- and intermolecular processes. While the most successful catalysts to date are derived from rhodium and copper, iridium catalysts also show promise. C–H insertion remains an active area of research and further developments are anticipated.

References

1 Ford, A., Miel, H., Ring, A. et al. (2015). *Chem. Rev.* 115: 9981.
2 White, M.C. (2012). *Synlett* 23: 2746.
3 Zheng, C. and You, S.-L. (2014). *RSC Adv.* 4: 6173.
4 Gillingham, D. and Fei, N. (2013). *Chem. Soc. Rev.* 42: 4918.
5 Davies, H.M.L. and Beckwith, R.E. (2003). *J. Chem. Rev.* 103: 2861.
6 Doyle, M.P., Duffy, R., Ratnikov, M., and Zhou, L. (2009). *Chem. Rev.* 110: 704.
7 Slattery, C.N., Ford, A., and Maguire, A.R. (2010). *Tetrahedron* 66: 6681.
8 Santiago, J.V. and Machado, A.H.L. (2016). *Beilstein J. Org. Chem.* 12: 882.
9 Demonceau, A., Noels, A.F., Hubert, A.J., and Teyssié, P. (1981). *J. Chem. Soc., Chem. Commun.* 688.
10 Wenkert, E., Davis, L.L., Mylari, B.L. et al. (1982). *J. Org. Chem.* 47: 3242.
11 Taber, D.F. and Petty, E.H. (1982). *J. Org. Chem.* 47: 4808.

12 Taber, D.F., Petty, E.H., and Raman, K. (1985). *J. Am. Chem. Soc.* 107: 196.

13 Pirrung, M.C. and Morehead, A.T. (1994). *J. Am. Chem. Soc.* 116: 8991.

14 Pirrung, M.C., Liu, H., and Morehead, A.T. (2002). *J. Am. Chem. Soc.* 124: 1014.

15 Nakamura, E., Yoshikai, N., and Yamanaka, M. (2002). *J. Am. Chem. Soc.* 124: 7181.

16 Yoshikai, N. and Nakamura, E. (2003). *Adv. Synth. Catal.* 345: 1159.

17 Hansen, J., Autschbach, J., and Davies, H.M.L. (2009). *J. Org. Chem.* 74: 6555.

18 Taber, D.F., You, K.K., and Rheingold, A.L. (1996). *J. Am. Chem. Soc.* 118: 547.

19 Doyle, M.P., Westrum, L.J., Wolthuis, W.N.E. et al. (1993). *J. Am. Chem. Soc.* 115: 958.

20 Davies, H.M.L., Hansen, T., and Churchill, M.R. (2000). *J. Am. Chem. Soc.* 122: 3063.

21 Ford, A. and Maguire, A.R. (2012). C—C bond formation (metal-carbene catalyzed). In: *Comprehensive Chirality*, vol. 4 (ed. E.M. Carreira and H. Yamamoto), 132. Amsterdam: Elsevier.

22 Doyle, M.P., Liu, Y., and Ratnikov, M. (2013). Catalytic, asymmetric, intramolecular carbon–hydrogen insertion. In: *Organic Reactions*, vol. 80 (ed. E.D. Scott), 1–132. Wiley.

23 Díaz-Requejo, M.M. and Pérez, P.J. (2008). *Chem. Rev.* 108: 3379.

24 Doyle, M.P., McKervey, M.A., and Ye, T. (1998). *Modern Catalytic Methods for Organic Synthesis with Diazo Compounds: From Cyclopropanes to Ylides.* New York: Wiley.

25 Maas, G. (1987). *Organic Synthesis, Reactions and Mechanisms*, 75. Springer.

26 Scott, L.T. and DeCicco, G.J. (1974). *J. Am. Chem. Soc.* 96: 322.

27 Lim, H.-J. and Sulikowski, G.A. (1995). *J. Org. Chem.* 60: 2326.

28 Desimoni, G., Faita, G., and Jørgensen, K.A. (2011). *Chem. Rev.* 111: PR284.

29 Slattery, C.N. and Maguire, A.R. (2011). *Org. Biomol. Chem.* 9: 667.

30 Flynn, C.J., Elcoate, C.J., Lawrence, S.E., and Maguire, A.R. (2010). *J. Am. Chem. Soc.* 132: 1184.

31 Axten, J.M., Ivy, R., Krim, L., and Winkler, J.D. (1999). *J. Am. Chem. Soc.* 121: 6511.

32 Hansen, J. and Davies, H.M.L. (2008). *Coord. Chem. Rev.* 252: 545.

33 Kennedy, M., McKervey, M.A., Maguire, A.R., and Roos, G.H.P. (1990). *J. Chem. Soc., Chem. Commun.* 361.

34 Davies, L. and Huw, M. (1999). *Eur. J. Org. Chem.* 1999: 2459.

35 Doyle, M.P., Zhou, Q.-L., Charnsangavej, C. et al. (1996). *Tetrahedron Lett.* 37: 4129.

36 Davies, H.M.L. and Beckwith, R.E.J. (2004). *J. Org. Chem.* 69: 9241. https://pubs.acs.org/doi/pdf/10.1021/jo048429m

37 Davies, H.M.L. and Panaro, S.A. (1999). *Tetrahedron Lett.* 40: 5287.

38 Qin, C. and Davies, H.M.L. (2014). *J. Am. Chem. Soc.* 136: 9792.

39 Qin, C., Boyarskikh, V., Hansen, J.H. et al. (2011). *J. Am. Chem. Soc.* 133: 19198.

40 Hashimoto, S.-I., Watanabe, N., and Ikegami, S. (1990). *Tetrahedron Lett.* 31: 5173.

41 Kitagaki, S., Anada, M., Kataoka, O. et al. (1999). *J. Am. Chem. Soc.* 121: 1417.

42 Reddy, R.P., Lee, G.H., and Davies, H.M.L. (2006). *Org. Lett.* 8: 3437.

43 Yamawaki, M., Tsutsui, H., Kitagaki, S. et al. (2002). *Tetrahedron Lett.* 43: 9561.

44 Tsutsui, H., Yamaguchi, Y., Kitagaki, S. et al. (2003). *Tetrahedron: Asymmetry* 14: 817.

45 Natori, Y., Ito, M., Anada, M. et al. (2015). *Tetrahedron Lett.* 56: 4324.

46 Fu, L., Wang, H., and Davies, H.M.L. (2014). *Org. Lett.* 16: 3036.

47 Dennis, A.M., Korp, J.D., Bernal, I. et al. (1983). *Inorg. Chem.* 22: 1522.

48 Timmons, D.J. and Doyle, M.P. (2005). Chiral dirhodium(II) catalysts and their applications. In: *Multiple Bonds Between Metal Atoms* (ed. F.A. Cotton, C.A. Murillo and R.A. Walton), 591–632.

49 Cotton, F.A., Barcelo, F., Lahuerta, P. et al. (1988). *Inorg. Chem.* 27: 1010.

50 Estevan, F., Herbst, K., Lahuerta, P. et al. (2001). *Organometallics* 20: 950.

51 Suematsu, H. and Katsuki, T. (2009). *J. Am. Chem. Soc.* 131: 14218.

52 Owens, C.P., Varela-Alvarez, A., Boyarskikh, V. et al. (2013). *Chem. Sci.* 4: 2590.

53 Wang, J.-C., Xu, Z.-J., Guo, Z. et al. (2012). *Chem. Commun.* 48: 4299.

54 Wang, J.-C., Zhang, Y., Xu, Z.-J. et al. (2013). *ACS Catal.* 3: 1144.

55 Chan, K.-H., Guan, X., Lo, V.K.-Y., and Che, C.-M. (2014). *Angew. Chem. Int. Ed.* 53: 2982.

56 Choi, M.K.-W., Yu, W.-Y., and Che, C.-M. (2005). *Org. Lett.* 7: 1081.

57 Taber, D.F. and Raman, K. (1983). *J. Am. Chem. Soc.* 105: 5935.

58 Padwa, A., Austin, D.J., Hornbuckle, S.F. et al. (1992). *J. Am. Chem. Soc.* 114: 1874.

59 Padwa, A., Austin, D.J., Price, A.T. et al. (1993). *J. Am. Chem. Soc.* 115: 8669.

60 Padwa, A. and Austin, D.J. (1994). *Angew. Chem. Int. Ed.* 33: 1797.

61 Cox, G.G., Moody, C.J., Austin, D.J., and Padwa, A. (1993). *Tetrahedron* 49: 5109.

62 Wee, A.G.H., Liu, B., and Zhang, L. (1992). *J. Org. Chem.* 57: 4404.

63 Taber, D.F. and Ruckle, R.E. (1986). *J. Am. Chem. Soc.* 108: 7686.

64 Shi, W., Zhang, B., Zhang, J. et al. (2005). *Org. Lett.* 7: 3103.

65 Doyle, M.P. and May, E.J. (2001). *Synlett* 0967.

66 Wamser, M. and Bach, T. (2014). *Synlett* 25: 1081.

67 Corey, E.J. and Felix, A.M. (1965). *J. Am. Chem. Soc.* 87: 2518.

68 Doyle, M.P., Protopopova, M.N., Winchester, W.R., and Daniel, K.L. (1992). *Tetrahedron Lett.* 33: 7819.

69 Doyle, M.P. and Kalinin, A.V. (1995). *Synlett* 1075.

70 Ring, A., Ford, A., and Maguire, A.R. (2016). *Tetrahedron Lett.* 57: 5399.

71 Doyle, M.P., Bagheri, V., Pearson, M.M., and Edwards, J.D. (1989). *Tetrahedron Lett.* 30: 7001.

72 McKervey, M.A. and Ye, T. (1992). *J. Chem. Soc., Chem. Commun.* 823.

73 Ito, M., Kondo, Y., Nambu, H. et al. (2015). *Tetrahedron Lett.* 56: 1397.

74 John, J.P. and Novikov, A.V. (2007). *Org. Lett.* 9: 61.

75 Jungong, C.S., John, J.P., and Novikov, A.V. (2009). *Tetrahedron Lett.* 50: 1954.

76 Taber, D.F., Paquette, C.M., Gu, P., and Tian, W. (2013). *J. Org. Chem.* 78: 9772.

77 Wolckenhauer, S.A., Devlin, A.S., and Du Bois, J. (2007). *Org. Lett.* 9: 4363.

78 Hinman, A. and Du Bois, J. (2003). *J. Am. Chem. Soc.* 125: 11510.

79 Jungong, C.S. and Novikov, A.V. (2013). *Tetrahedron: Asymmetry* 24: 151.

80 Rosales, A., Rodríguez-García, I., López-Sánchez, C. et al. (2011). *Tetrahedron* 67: 3071.

81 Taber, D.F. and Ruckle, R.E. (1985). *Tetrahedron Lett.* 26: 3059.

82 Doyle, M.P., Dyatkin, A.B., Roos, G.H.P. et al. (1994). *J. Am. Chem. Soc.* 116: 4507.

83 Doyle, M.P., Zhou, Q.-L., Dyatkin, A.B., and Ruppar, D.A. (1995). *Tetrahedron Lett.* 36: 7579.

84 Müller, P. and Polleux, P. (1994). *Helv. Chim. Acta* 77: 645.

85 Doyle, M.P., Dyatkin, A.B., Protopopova, M.N. et al. (1995). *Recl. Trav. Chim. Pays-Bas* 114: 163.

86 Doyle, M.P., Kalinin, A.V., and Ene, D.G. (1996). *J. Am. Chem. Soc.* 118: 8837.

87 DeAngelis, A., Dmitrenko, O., Yap, G.P.A., and Fox, J.M. (2009). *J. Am. Chem. Soc.* 131: 7230.

88 Lindsay, V.N.G., Lin, W., and Charette, A.B. (2009). *J. Am. Chem. Soc.* 131: 16383.

89 Doyle, M.P., Morgan, J.P., Fettinger, J.C. et al. (2005). *J. Org. Chem.* 70: 5291.

90 Rasappan, R., Laventine, D., and Reiser, O. (2008). *Coord. Chem. Rev.* 252: 702.

91 Shiely, A.E., Slattery, C.N., Ford, A. et al. (2017). *Org. Biomol. Chem.* 15: 2609.

92 Slattery, C.N. and Maguire, A.R. (2013). *Tetrahedron Lett.* 54: 2799.

93 Bode, J.W., Doyle, M.P., Protopopova, M.N., and Zhou, Q.-L. (1996). *J. Org. Chem.* 61: 9146.

94 Doyle, M.P. and Hu, W. (2002). *Chirality* 14: 169.

95 Anada, M., Mita, O., Watanabe, H. et al. (1999). *Synlett* 1775.

96 Natori, Y., Tsutsui, H., Sato, N. et al. (2009). *J. Org. Chem.* 74: 4418.

97 Wu, W.-T., Yang, Z.-P., and You, S.-L. (2015). Asymmetric C–H Bond Insertion Reactions. In: *Asymmetric Functionalization of C—H Bonds* (ed. S.-L. You), 1. The Royal Society of Chemistry.

98 Liao, K., Negretti, S., Musaev, D.G. et al. (2016). *Nature* 533: 230.

99 Davies, H.M.L. and Denton, J.R. (2009). *Chem. Soc. Rev.* 38: 3061.

100 Müller, P. and Tohill, S. (2000). *Tetrahedron* 56: 1725.

101 Goto, T., Onozuka, T., Kosaka, Y. et al. (2012). *Heterocycles* 86: 1647.

102 Davies, H.M.L., Huby, N.J.S., Cantrell, W.R., and Olive, J.L. (1993). *J. Am. Chem. Soc.* 115: 9468.

103 Davies, H.M.L., Beckwith, R.E.J. (2004). *J. Org. Chem.* 69: 9241. (https://pubs.acs.org/doi/10.1021/jo048429m)

104 Davies, H.M.L. and Walji, A.M. (2005). *Angew. Chem. Int. Ed.* 44: 1733.

105 Davies, H.M.L., Coleman, M.G., and Ventura, D.L. (2007). *Org. Lett.* 9: 4971.

106 Ventura, D.L., Li, Z., Coleman, M.G., and Davies, H.M.L. (2009). *Tetrahedron* 65: 3052.

107 Davies, H.M.L. and Yang, J. (2003). *Adv. Synth. Catal.* 345: 1133.

108 Fraile, J.M., García, J.I., Mayoral, J.A., and Roldán, M. (2007). *Org. Lett.* 9: 731.

109 Davies, H.M.L., Beckwith, R.E.J., Antoulinakis, E.G., and Jin, Q. (2003). *J. Org. Chem.* 68: 6126.

110 Davies, H.M.L. and Morton, D. (2011). *Chem. Soc. Rev.* 40: 1857.

111 Davies, H.M.L. and Venkataramani, C. (2002). *Angew. Chem. Int. Ed.* 41: 2197.

112 Guptill, D.M. and Davies, H.M.L. (2014). *J. Am. Chem. Soc.* 136: 17718.

113 Davies, H.M.L., Ren, P., and Jin, Q. (2001). *Org. Lett.* 3: 3587.

114 Davies, H.M.L., Hansen, T., Hopper, D.W., and Panaro, S.A. (1999). *J. Am. Chem. Soc.* 121: 6509.

115 Davies, H.M.L., Stafford, D.G., Hansen, T. et al. (2000). *Tetrahedron Lett.* 41: 2035.

116 Reddy, R.P. and Davies, H.M.L. (2006). *Org. Lett.* 8: 5013.

117 Davies, H.M.L. and Jin, Q. (2003). *Tetrahedron: Asymmetry* 14: 941.

118 Davies, H.M.L. and Ni, A. (2006). *Chem. Commun.* 3110.

119 Davies, H.M.L., Walji, A.M., and Townsend, R.J. (2002). *Tetrahedron Lett.* 43: 4981.